Università degli studi di Padova

Dipartimento di Scienze Chirurgiche Oncologiche e Gastroenterologiche

---

CORSO DI DOTTORATO DI RICERCA IN ONCOLOGIA CLINICA E SPERIMENTALE E IMMUNOLOGIA

CICLO XXXII

The mitochondrial Ca^{2+} homeostasis in breast cancer

Coordinatore: Ch.mo Prof.ssa Paola Zanovello

Supervisore: Ch.mo Prof. Simone Mocellin

Co-Supervisore: Ch.mo Prof.ssa Cristina Mammucari

Dottorando: Halenya Monticelli

Table of contents

SUMMARY

Breast cancer is the most common invasive cancer among women, affecting about 12% of all new cancer cases and it is the first leading cause of cancer-related death in women worldwide [International Agency for Cancer Research]. Triple-negative breast cancer (TNBC) represents one of the most aggressive breast tumour subtypes but the molecular mechanisms promoting tumour aggressiveness is still undefined. Several findings indicate that cancer cells undergo a complex metabolic reprogramming to satisfy the increased requirement of macromolecules and energy necessary for proliferation, and mitochondria have a fundamental role in this mechanism. Indeed, mitochondria are producers of intermediates for lipid, nucleic acid, and protein synthesis but also players of control of the cell fate. In these processes, mitochondrial calcium plays a pivotal role: in physiological conditions, it directly regulates three enzymes of the TCA cycle, i.e. pyruvate-, α-ketoglutarate- and isocitrate-dehydrogenases (Berridge et al., 2000); while in pathological conditions, mitochondrial Ca^{2+} overload sensitizes cells to apoptotic challenges by triggering the opening of the mitochondrial permeability transition pore (mPTP) (Basso et al., 2005)

The channel responsible for entry into the mitochondria is the mitochondrial calcium uniporter (MCU) (Baughman et al., 2011; De Stefani et al., 2011) that is composed of both channel-forming subunits and regulatory proteins. In addition to MCU, MCUb, the dominant-negative isoform of MCU (Raffaello et al., 2013), and the essential MCU regulator EMRE (Sancak et al., 2013) contribute to channel formation. The MICU protein family, comprising MICU1, MICU2 and MICU3, regulates the sophisticated mechanism of mitochondrial calcium uptake by modulating MCU function (De Stefani et al., 2016). While MICU3 expression is mainly confined to the nervous system, MICU1 and MICU2 are ubiquitous. MICU1 and MICU2 form a regulatory heterodimer that finely tunes MCU activity. Within the heterodimer, MICU1

increases and MICU2 reduces MCU activity. Both MICU1 and MICU2 possess EF-hand domains that bind Ca^{2+} ions. At low extra-mitochondrial [Ca^{2+}], MICU2 plays a dominant effect thus inhibiting MCU activity. At higher extra-mitochondrial [Ca^{2+}], MICU1 exerts a stimulatory effect allowing the prompt response of mitochondria to cytosolic [Ca^{2+}] rises.

It was already demonstrated that genetic inhibition of MCU expression causes a significant decline in TNBC metastatic cell motility and invasiveness (Tosatto et al., 2016) and hampers metastasis formation *in vivo*.

To further understand the role of the mitochondrial Ca^{2+} uptake in TNBC, and to explore possible therapeutic targets, we aimed to study the role of the MICU1 and MICU2 in TNBC progression, both *in vitro* and *in vivo.* Firstly, we detected a decrease in MICU1 expression levels in tumour samples compared to normal breast samples underlining the importance of mitochondrial Ca^{2+} uptake in breast tumour development. Then, we demonstrated that the mitochondrial Ca^{2+} uptake inhibition, by overexpression ofMICU1 and MICU2 isoforms in which the EF-hands are mutated in order to hamper Ca^{2+} binding, causes a significant decline in TNBC cell motility *in vitro* and in tumour growth and metastasis formation *in vivo*. In these conditions, mROS production was significantly reduced, suggesting that mROS might play a crucial role in MICU1/2 dependent control of malignancy.

In the second part of the thesis, we studied the role of MCUb, the dominant-negative isoform of MCU. While MCU expression increases with tumour progression, the expression of MCUb decreases (Tosatto et al., 2016). Thus, we decided to overexpress MCUb in a TNBC cell line. Overexpression of MCUb partially inhibits tumour cell growth. Moreover, MCUb overexpression causes a significant decline in TNBC cell motility.

Our results highlight a crucial role of the mitochondrial Ca^{2+} uptake in the control of TNBC metastatic potential and indicate that the MCU regulatory subunits and MCUb could represent novel therapeutic target for clinical intervention.

RIASSUNTO

I tumori mammari rappresentano la forma di tumore più frequente nella popolazione femminile, con un'incidenza del 12% dei nuovi casi di tumore e una mortalità del 15% [IACR; gco.iarc.fr]. Il carcinoma mammario triplo negativo (dall'inglese TNBC) è una delle classi più aggressive ed eterogenee, caratterizzato dalla mancata espressione dei recettori estrogenici, progestinici ed HER2 ma ad oggi non sono del tutto noti i meccanismi molecolari che promuovono l'aggressività tumorale. Diverse evidenze indicano che le cellule tumorali subiscono un complesso rimodellamento del metabolismo per soddisfare il maggiore bisogno di macromolecole ed energia necessarie per la proliferazione. La riprogrammazione del metabolismo mitocondriale è un aspetto chiave in questi meccanismi. Infatti, i mitocondri partecipano alla produzione di intermedi lipidici, di acidi nucleici e alla sintesi di proteine ma allo stesso tempo possono influire sulla morte cellulare. In tutti questi processi, il flusso di Ca^{2+} mitocondriale è il principale regolatore della bioenergetica cellulare: in condizioni fisiologiche infatti, controlla tre enzimi del ciclo di Krebs; i.e. piruvato-, α-ketoglutarato- e isocitrato deidrogenasi (Berridge et al., 2000); mentre un sovraccarico di Ca^{2+} nel mitocondrio porta inevitabilmente ad una disfunzione dell'organello e apertura del Poro di Transizione della Permeabilita (PTP), seguita dall'apoptosi e quindi dalla morte cellulare (Basso et al., 2005).

L'Uniporto Mitocondriale del Calcio (MCU) è un canale altamente selettivo per il Ca^{2+} che regola l'ingresso di Ca^{2+} all'interno della matrice. Oltre a MCU, contribuiscono alla formazione del canale l'isoforma dominante negativa di MCU, MCUb (Raffaello et al., 2013) e la proteina strutturale EMRE (Sancak et al., 2013). Le subunità regolatorie comprendono MICU1, MICU2 e MICU3 (De Stefani et al., 2016) e hanno il ruolo di modulare le funzioni di MCU. Infatti, MICU1 e MICU2 formano un eterodimero che modula finemente l'attività di MCU. Entrambe le proteine sono caratterizzate dalla presenza di domini che legano il calcio (domini EF-hand).

A basse [Ca^{2+}] MICU2 svolge un'azione inibitoria mentre ad alte [Ca^{2+}] MICU1 svolge un'azione stimolatrice, permettendo al mitocondrio di rispondere rapidamente ai cambiamenti di Ca^{2+} citosolico.

In un precedente lavoro, è stato dimostrato che l'inibizione genetica di MCU riduce la migrazione di cellule tumorali in vitro e la formazione di metastasi in vivo (Tosatto et al., 2016). Al fine di caratterizzare ulteriormente il ruolo del Ca^{2+} mitocondriale nel TNBC, e al fine di scoprire nuovi target terapeutici, in questo studio si è deciso di investigare il ruolo di MICU1 e MICU2 nella progressione del TNBC, sia in vitro che in vivo. Uno studio di espressione proteica ci ha permesso di evidenziare una diminuita espressione di MICU1 in campioni di tumore mammario rispetto a campioni sani. Questo dato sottolinea l'importanza dell'accumulo di Ca^{2+} mitocondriale per la progressione del tumore mammario. A questo punto abbiamo dimostrato che l'inibizione di accumulo di Ca^{2+} mitocondriale, mediante l'espressione di MICU1 e MICU2 mutati nei domini EF-hand, causa un declino significativo della motilità di cellule TNBC in vitro e una diminuita crescita tumorale e formazione di metastasi in vivo. Si è deciso di investigare come queste condizioni contribuiscano alla produzione mitocondriale di specie radicaliche dell'ossigeno (ROS) e abbiamo verificato che la produzione di ROS è significativamente ridotta, suggerendo così che i ROS mitocondriali giocano un ruolo cruciale nella regolazione della malignità tumorale mediata dal Ca^{2+}mitocondriale.

Nella seconda parte della tesi, abbiamo studiato il ruolo di MCUb, l'isoforma dominante negativa di MCU. Mentre l'espressione di MCU aumenta con la progressione tumorale, l'espressione di MCUb diminuisce (Tosatto et al., 2016). Per questo abbiamo deciso di overesprimere MCUb in cellule di TNBC. L'overespressione di MCUb inibisce in parte la crescita tumorale e causa una sigificativa diminuizione della motilità di cellule TNBC.

In conclusione i nostri risultati evidenziano il ruolo cruciale del flusso di calcio mitocondriale nel controllo del potenziale metastatico del tumore mammario triplo negativo ed indicano che

le subunità regolatorie di MCU e MCUb rappresentano un nuovo bersaglio terapeutico per un innovativo approccio clinico.

INTRODUCTION

Metabolic reprogramming: a hallmark of cancer

Cancer is a heterogeneous disease, both biologically and clinically, with distinct histological and genetic features. In 2018, 18 million new cancer cases and 9,5 million cancer-related deaths have been estimated. Among all cancers, lung and breast are the most frequently diagnosed cancers and the leading causes of cancer death in men and women, respectively (International Agency for Cancer Research, www.iarc.fr). During the year 2000, Hanahan and Weinberg published their milestone review (Hanahan and Weinberg, 2000) in which they organized the complexity of cancer biology in six hallmarks: self-sufficiency in growth signals, insensitivity to antigrowth signals, evasion of apoptosis, undefined replicative potential, sustained angiogenesis, tissue invasion and metastasis. Years later other four hallmarks were added: reprogramming energy metabolism and evading the immune response, genome instability and mutation, and tumour-promoting inflammation, giving a higher grade of complexity to cancer biology (Hanahan et al., 2011).

Here, I will focus on one of the new hallmarks: the reprogramming of energy metabolism.

In 1927, Otto Warburg reported that cancer cells undergo a complex metabolic reprogramming to satisfy the increased requirement of macromolecules and energy necessary for proliferation (Warburg et al., 1927). He observed that cancer cells consume large amounts of glucose through glycolysis even in the presence of oxygen, whereas normal cells predominantly use respiration. He further hypothesized that cancer transformation was caused by inherent defects in mitochondrial function (Warburg, 1956). Despite debated, Warburg's observations prompted to understand the biochemical determinants of cancer transformation (Weinhouse, 1976). The link between metabolism and cancer progression was further corroborated in the early 2000s, by the discovery that mutations of housekeeping metabolic enzymes such as succinate

dehydrogenase (SDH) (Baysal, 2003)and fumarate hydratase (FH) (Tomlinson et al., 2002) were associated with hereditary forms of cancer. These findings highlighted the possibility that altered metabolism could be the cause of cancer transformation. Further studies demonstrated that respiration is not impaired in most cancer cells but the switch to aerobic glycolysis in cancer cells is functional to support the anabolic requirements associated with cell growth and proliferation, providing glycolytic intermediates for biosynthesis (Heiden et al., 2009). These efforts culminated with the discovery that a huge number of oncogenes and tumour suppressors are implicated in the regulation of cancer cell metabolism (e.g. Ras and Akt mutations increase glycolytic flux at different levels (Hsu and Sabatini, 2008)) and that key metabolic enzymes if mutated, predispose to cancer.

Finally, Pavlova and Thompson underlined that the metabolic alterations associated with the tumorigenesis, involve all stages of the cell-metabolite interaction. Their analysis showed that cancer affects: i) the metabolite influx through a deregulated uptake of glucose and amino acids, and through opportunistic modes of nutrient acquisition; ii) the intracellular metabolism by aberrant utilization of glycolysis and TCA (tricarboxylic acid cycle) cycle intermediates for biosynthesis and NADPH production; iii) cellular behavior and fate by long-ranging effects of metabolic reprogramming on the cancer cell itself, as well as on other cells within its microenvironment (Pavlova and Thompson, 2016).

A factor required for the metastatic propagation is the optimal mitochondrial biogenesis and efficient oxidative phosphorylation. Furthermore, mitochondria are not only sources of energy and producers of macromolecules intermediates but also a key controller of cell fate. PGC-1α silencing in cell models of breast cancer cells abrogates their invasive potential and metastasis ability without affecting proliferation (LeBleu et al., 2014). It is known the role of mitochondria in metabolic switches involved in cancer progression but the metabolic switch seems to be

reversible, and mitochondria remain functional and mutation-free in many cases following cancerous transformation (Vyas et al., 2016).

It is now clear that metabolic reprogramming is an obligate step of cancer transformation, required to sustain unrestrained proliferation triggered by the activation of oncogenic signalling cascades, which turns tumour metabolism to a hallmark of cancer.

Aerobic glycolysis

Non-proliferating cells of differentiated tissues predominantly use mitochondrial oxidative phosphorylation (OXPHOS) to fuel their energetic needs. In contrast, highly proliferative tissues, as well as cancer cells, are characterized by high glucose utilization, lactate production and biosynthesis of macromolecules, giving rise to metabolic pathways shift toward an anabolic metabolism (Figure 1) (Fritz and Fajas, 2010). In 1956, Warburg defined aerobic glycolysis as the metabolic process that converts glucose into lactate even under aerobic conditions, and initially, the induction of aerobic glycolysis in tumour cells was thought to be caused by inherent mitochondrial dysfunction (Warburg, 1956). However, it is now clear that respiration is not impaired in most cancer cells and that aerobic glycolysis is functional also in non-transformed cells, such as activated lymphocytes and embryonic stem cells (Zhang et al., 2012), indicating that aerobic glycolysis can be considered a common metabolic phenotype (metabotype) of proliferating cells.

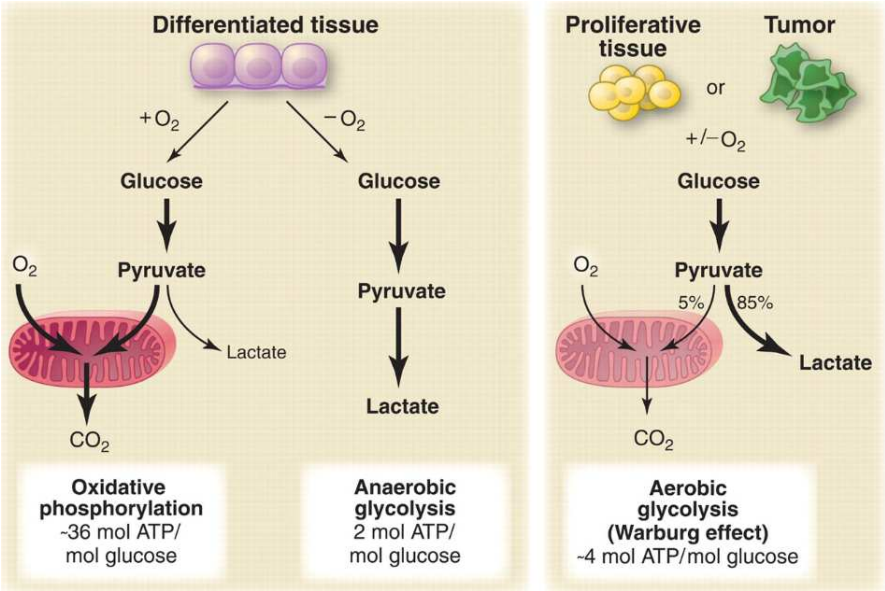

Figure 1: **Schematic representation of oxidative phosphorylation, anaerobic glycolysis and aerobic glycolysis** (Vander Heiden et al., 2009): in the presence of oxygen, differentiated tissues metabolize glucose to pyruvate via glycolysis and then completely oxidize pyruvate in the mitochondria to CO_2 and H_2O during the process of oxidative phosphorylation. In hypoxic condition, cells can shift toward anaerobic glycolysis by the generation of lactate from pyruvate produced by glycolysis. The generation of lactate allows glycolysis to continue but results in minimal ATP production when compared with oxidative phosphorylation. Warburg observed that cancer cells tend to convert most glucose to lactate regardless of whether oxygen is present

Glycolysis generates 2 molecules of ATP per molecule of glucose converted in pyruvate, whereas the full oxidation of glucose by mitochondria generates 31 molecules of ATP. Based on pure stoichiometric calculations, aerobic glycolysis is an inefficient pathway for ATP generation, and the switch to this metabotype seems a paradox for cancer cells. However, the use of aerobic glycolysis offers some advantages to highly proliferative cells: indeed glucose is the most abundant extracellular nutrient and from a kinetic point of view, glycolysis is not an inefficient process because it can generate ATP in a fast rate when glucose is provided at a sufficiently high concentration (Pfeiffer et al., 2001): the glycolytic flux is so efficient in cancer cells compared to non-transformed cells that, by the time one molecule of glucose is fully oxidized via respiration, 24 additional ATPs are generated via aerobic glycolysis demonstrating that aerobic glycolysis could still supply 2/3 of the ATP (Koppenol et al., 2011).

Finally, glucose degradation provides cells with intermediates needed for biosynthetic pathways, including ribose sugars for nucleotides, glycerol and citrate for lipids and

nonessential amino acids (Heiden et al., 2009). Given the large amount of glucose taken up by cancer cells in the unit time, it has been speculated that the amount of ATP generated by aerobic glycolysis might even exceed the ATP requirements of cancer cells (Racker, 1976). In proliferating cells, low ATP/ADP ratios are necessary to maintain enhanced glycolysis, which can occur if mitochondrial metabolism is altered. Indeed, without sufficient ATP turnover, ADP and phosphate would become limiting factors for glycolysis, and the accumulation of ATP would cause the allosteric inhibition of key metabolic enzymes, such as phosphofructokinase (PFK1), blocking the entire glycolytic flux. Otherwise different studies show the evidence that ATP may never be limiting in cancer cells. Despite the stimulation to divide, cells using aerobic glycolysis also exhibit high ratios of ATP/ADP and NADH/NAD+ (Christofk et al., 2008; DeBerardinis et al., 2008). Recently, an example of cancer-specific ATP-consuming reactions has been reported: the expression of the cancer-specific M2 variant of pyruvate kinase (PKM2), which was shown to uncouple pyruvate production from ATP generation, by stimulating the transfer of the high-energy phosphate of phosphoenolpyruvate to the glycolytic enzyme phosphoglycerate-mutase (PGAM), instead of ADP (Vander Heiden et al., 2010). However, the molecular mechanisms responsible for aerobic glycolysis shift remain an exciting scientific challenge.

Mitochondria metabolism and cell migration

Cell migration is a process finalized to the invasion of the surrounding tissues and metastasis dissemination whereby cancer will colonize and form macroscopic lesions at distant sites (López-Soto et al., 2017). One of the first alterations of these processes is the epithelial-to-mesenchymal transition (EMT), that is the process by which epithelial cells lose their cell polarity and cell-cell adhesion to gain invasive proprieties becoming mesenchymal cells.

Several mitochondrial metabolites participate in the EMT (Gaude and Frezza, 2014). Indeed, defect of mitochondrial enzymes could deregulate cellular energetics as in the case of fumarate hydratase (FH), succinate dehydrogenase (SDH), and isocitrate dehydrogenase (IDH) (Gaude and Frezza, 2014). SDH and FH act as tumour suppressors in normal cells but a mutation in both was discovered in cancer cells inducing an accumulation of succinate or fumarate (Aspuria et al., 2014).

FH deficiency is associated with a highly aggressive phenotype in renal carcinoma that leads to metastasis formation. Moreover, fumarate accumulation caused by the loss of FH is associated with the induction of EMT in mouse and human cells by suppressing the anti-metastatic miRNA miR-200 and activating EMT-transcription factors (Sciacovelli and Frezza, 2017).

SDH is an enzyme complex bound to the inner mitochondrial membrane that converts succinate into fumarate, but it is the only known enzyme of the respiratory chain completely encoded by nuclear DNA without having proton pumping activity. Inactivating mutations of SDH subunits and assembly factors have been linked to different types of hereditary and sporadic forms of cancers. SDH mutations lead to an accumulation of succinate which the oncogenic role is linked to the inhibition of PHD (HIF-α prolyl hydroxylase) and the subsequent stabilization of hypoxia-inducible factor (HIF1α) (Selak et al., 2005). A further study found succinate to be an 'epigenetic hacker', capable of inhibiting both DNA and histone demethylases (Yang and Pollard, 2013).

IDH is also a mitochondrial enzyme involved in EMT. IDH catalyzes the oxidative decarboxylation of isocitrate to α-ketoglutarate. Gain-of-function mutations were found in IDH1/2. These mutant forms convert α-ketoglutarate to 2-hydroxyglutarate (2HG), which may contribute to the inhibition of DNA demethylases and aberrant regulation of gene expression patterns (Figueroa et al., 2010). IDH1/2 mutations induce the accumulation of 2-HG leading to EMT by zinc finger E-box-binding homeobox 1 (ZEB1) upregulation and miR-200

downregulation in breast tumours and colorectal cancer cells (Grassian et al., 2012). The tumourigenic activity of 2HG has been attributed to its inhibitory effect on various oxoglutarate-dependent dioxygenases, including the PHD, histone demethylases, and the teneleven translocation (TET) family of DNA demethylases (Chowdhury et al., 2011).
Furthermore, it is important to consider the heterogeneity of cancer and cancer metastasis and the fact that they can rely on glycolytic or respiratory metabolism differently depending on their different origin (Mayers et al., 2016)or different anatomical location (Dupuy et al., 2015).

Reactive oxygen species

Oxygen is an indispensable molecule for the aerobic organisms. However, Reactive Oxygen Species (ROS), which are generated by partial O_2 reduction, can be formed by a variety of mechanisms, including generation during oxidative phosphorylation in the mitochondria, as a byproduct of normal cellular aerobic metabolism (Davies, 1995). The partial oxygen reduction can produce several products: one of the most abundant ROS produced in mitochondria is the superoxide anion radical that has a high oxidative capacity and it is a by-product of oxygen metabolism. The mos t potent and aggressive oxidant primarily responsible for oxidative damage of DNA bases is the hydroxyl radical, which has a relatively short half-life but virtually can damage all types of macromolecules. Singlet oxygen is commonly formed following exposure to UV or visible light in the presence of chromophores that can act as sensitizing agents and it interacts with a wide range of biological targets, including DNA, RNA, proteins, lipids and sterols (Davies, 2003). Superoxide anion has biological toxicity because of its capacity to inactivate iron-sulfur cluster containing enzymes, critical in a wide variety of metabolic pathways, thereby liberating free iron in the cell, which can generate the highly reactive hydroxyl radical.

In mitochondria, ROS are generated during oxidative phosphorylation as a product of normal cellular aerobic metabolism (Davies, 1995). Indeed, in the aerobic environment, mitochondrial ATP generation is coupled to the reduction of molecular oxygen to water and electron transport in the respiratory chain. ROS are principally formed by complex I and III in which free electrons responsible for ROS generation are released by the oxidation of high energy molecules, such as NADH and FAD, and carried by "electron carriers" such as Coenzyme Q and Cytochrome C (Davies, 1995). From what discuss above, ROS homeostasis results fundamental for cell survival and normal cell signalling, preventing cells from damage. Detoxification of ROS is achieved by non-enzymatic or enzymatic antioxidant systems which are involved in scavenging of different types of ROS. Non-enzymatic molecules include glutathione, flavonoids, vitamin A, C and E. Enzymatic antioxidants include superoxide dismutase (SOD), superoxide reductase, catalase, glutathione peroxidase (GPX), glutathione reductase, peroxiredoxin (PRX) and thioredoxin (TRX) (Tan et al., 2018).

Deregulation of mitochondrial ROS can result in the initiation and progression of various cancer types. Indeed, different levels of oxidative stress appear to confer different outcomes in cancer cells: while high oxidative stress can lead to cell death (Nishikawa, 2008), mild oxidative stress at sub-lethal levels could activate pro-survival signalling pathways, loss of tumour suppressor gene-function, increased glucose metabolism, adaptations to hypoxia and the generation of oncogenic mutations (Moloney and Cotter, 2018). The main function of antioxidant defences is to maintain a reduction-oxidation (redox) balance: indeed, on one hand, the antioxidant capacity of tumour cells scavenges excessive ROS, on the other it maintains pro-tumourigenic ROS levels, allowing the disease to progress and develop resistance to apoptosis (Gorrini et al., 2013). Moreover, due to their reactive chemical nature, ROS are capable of attacking various components of DNA, leading to the generation of a variety of ROS-mediated modified product that could increase the risk of developing drug-resistant cancer cells

(Pelicano et al., 2004). On the contrary, toxic levels of ROS production in cancers causes an increase of oxidative stress and, eventually, cell death. Thus, high levels of ROS are anti-tumourigenic factors (Nogueira et al., 2008).

Here we will analyze the main ROS-triggered events involved in cancer progression: cell adhesion, cell invasion and migration, epithelial-to-mesenchymal-transition (Figure 2).

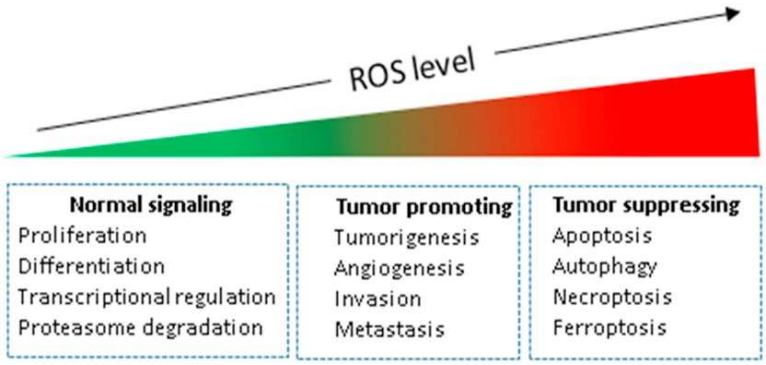

Figure 2: **Role of ROS in biological processes** (Galadri et al. 2017)
Cancer cells have an inherent elevated ROS level compared to their normal counterparts. Elevated oxidative signalling may be implicated in the promotion and progression of a number of different cancers. In addition, increased ROS levels have been linked to cancer initiation, malignant transformation, and resistance to chemotherapy. Despite this, increased ROS levels in cancer cells may provide a unique opportunity to eliminate cancer cells via elevating ROS to highly toxic levels intracellularly, thereby, activating various ROS-induced cell death pathways, or inhibiting cancer cell resistance to chemotherapy.

Cell adhesion: The role of ROS in cell adhesion is well established since many integrins signalling are accompanied by a mild oxidative burst. Although the underlying molecular mechanisms remain to be precisely defined, there is clear evidence that integrins engagement with antibodies or extracellular matrix proteins triggers ROS production by promoting changes in mitochondrial metabolic/redox function (Werner and Werb, 2002), and activation of distinct oxidases, including NADPH-oxidases (Chiarugi et al., 2003), and the AA-metabolizing enzymes 5-lipoxygenase (5-LOX) (Taddei et al., 2007). One of the most well-studied focal adhesion protein is focal adhesion kinase (FAK), the principal kinase responsible for the formation of focal adhesion complexes (Mahdi et al., 2001). Interactions between FAK and Src kinase have been implicated in crucial roles in cell migration by phosphorylating the focal adaptor proteins protein kinase C (PKC). The integrins signalling activates PKC, which in turn

can signal back to activate integrins, suggesting the presence of a positive feedback mechanism between integrin and PKCs (Disatnik and Rando, 1999). Recently, ROS have been identified as intermediate players in this loop. Indeed, in a hepatocellular carcinoma model, the translocation of PKC to the cell membrane activates integrins signalling that results in increased ROS levels. The ROS thus generated oxidize PKC and activate it. Thus, PKC-dependent integrin signalling generates ROS, which may, in turn, re-activate PKC, leading to sustained ERK activation (Hu et al., 2011).

Cell invasion and migration: ROS target several major signalling molecules, including kinases and transcription factors, which are known to be involved in invasion and migration of cancer cells. When generated as a result of growth factor receptor stimulation, ROS trans signals to induce cellular changes necessary for migration. It is reported that endogenous catecholamines such as adrenaline and noradrenaline produce ROS and promoted the invasion of MDA-MB-231 human breast cancer cells through β2-adrenergic signalling (Yamazaki et al., 2014).

Members of the Mitogen-Activated Protein Kinase (MAPK) family are activated during cell migration. One mechanism by which ROS mediate activation of these pathways is via growth factor stimulation of receptor tyrosine kinases (RTKs) (Wu, 2006).

Furthermore, in endothelial cells, NOX activity was shown to correlate with ROS production, leading to enhanced cell tumorigenesis and invasion. Indeed, it was shown that in lung cancer NOX activity and expression are associated with tumorigenesis. Moreover, the inhibition of NOX mRNA expression significantly blocks lung cancer formation and invasion (Han et al., 2016).

Important signalling targets of ROS during cell migration include the protein kinase C (PKCs) as well as the protein tyrosine phosphatases (PTPs) (Wu, 2006). Indeed, both PKCs and PTPs

contain critical cysteine residues that can be oxidized by ROS. PKCs are activated upon oxidation while PTPs are inhibited. Thus, the oxidation of PKCs and PTPs can activate the MAPK signalling cascade leading to tumour cell migration (Boivin et al., 2010). As already discussed for the cellular adhesion mechanism, activated PKC, in turn, can influence ROS generation, suggesting the existence of a positive feedback mechanism from ROS to PKC and vice versa, resulting in signal amplification that enhances cell migration (Boivin et al., 2010). Different types of cellular protrusions have been described during cell migration, including filopodia, lamellipodia, and invadopodia. Formation of specific protrusions is regulated by signalling pathways; for example, Rho activation induces filopodia and stress fiber formation, while induction of Rac leads to the formation of lamellipodia and membrane ruffles (Nobes and Hall, 1999). These cellular protrusions are affected by dynamic alterations in the actin cytoskeleton, which in turn is controlled by signalling molecules such as Rac. Rac has been identified as an upstream regulator of the ROS-producing enzyme Nox, indicating that a pathway exists for ROS-regulation of the actin cytoskeleton. Furthermore, ROS production increased the expression of MMP-2 and MMP-9, which is regulated by CLIC1-mediated invasion of cells (Wang, 2014).

Epithelial-to-mesenchymal-transition (EMT): EMT is the process by which an epithelial cell attains a mesenchymal phenotype. This is accompanied by loss of epithelial markers (including E-cadherin, laminin 1, ZO-1, cytokeratin, and collagen IV), induction of mesenchymal markers (such as N-cadherin and vimentin) and upregulation of transcription factors that promote the transition from epithelial to mesenchymal cells (Snail, Slug, Twist, NF-κB, and Zeb). EMT is recognized as driving force of cancer cell metastasis and drug resistance, and ROS have been widely documented to participate in the induction of EMT in cancer, mainly through the activation of Snail (Cannito et al., 2008). At the same time Snail overexpression increases

intracellular ROS levels in prostate cancer (Barnett et al., 2011). In mammary epithelial cells, the overexpression of MMP-3 induces the expression of an alternatively spliced form of Rac1, which causes an increase in cellular reactive oxygen species (ROS). ROS stimulates the expression of the transcription factor Snail and EMT, and cause oxidative damage to DNA and genomic instability (Radisky et al., 2005).

These data suggest a possible feedback mechanism by which ROS and Snail can regulate each other and lead to the induction of EMT.

Mounting evidence also suggests the influence of TGF-beta induced ROS in EMT-mediated cellular changes. As a multi-potent cytokine, TGF-beta plays an important role in EMT and tumour progression. Several mechanisms by which TGF-beta induces EMT via regulation of intracellular ROS have been proposed. TGF-beta has been shown to increase ROS levels by decreasing the expression and activity of the antioxidant protein Glutaredoxin (Grx1) (Lee et al., 2010). In mammary epithelial cells expressing oncogenic Ras, downregulation of Grx1 by TGF-beta leads to increased intracellular ROS levels promoting EMT. Moreover, increased ROS levels downstream of TGF-beta have been shown to activate signalling pathways such as MAPK leading to EMT (Felton et al., 2009).

Ca^{2+} signalling

Mitochondria Ca^{2+} signalling

Mitochondria represent a unique organelle within the complex endomembrane systems that characterize any eukaryotic cell. Beyond the pivotal role they play in ATP production, a whole new mitochondrial biology has emerged in the last few decades: mitochondria have been shown to participate in many other aspects of cell physiology such as amino-acid synthesis, iron-sulphur clusters assembly, lipid metabolism, Ca^{2+} signalling, reactive oxygen species (ROS) production and cell death regulation. Hence, many pathological conditions are associated with mitochondria dysfunction, including neurodegenerative diseases (Alzheimer's, Parkinson's, Huntington's), motoneuron disorders (amyotrophic lateral sclerosis, type 2A Charcot-Marie-Tooth neuropathy), autosomal dominant optic atrophy, ischemia-reperfusion injury, diabetes, ageing and cancer (Gaude and Frezza, 2014). Mitochondria are defined by two structurally and functionally different membranes: outer membrane (OMM) and the inner membrane (IMM), characterized by invaginations called "cristae", which enclose the mitochondrial matrix. The space between these two structures is traditionally called intermembrane space (IMS), but recent advances in electron microscopy techniques have shed new light on the complex topology of the inner membrane. Cristae indeed are not simply random folds, but rather internal compartments are formed by profound invaginations, originating from very tiny "point-like structures" in the inner membrane (Mannella, 2006). These narrow tubular structures, called cristae junctions, can limit the diffusion of the molecules from the intra-cristae space towards the IMS, thus creating a micro-environment where respiratory chain complexes, and also other proteins, are hosted and protected from random diffusion. The OMM contains a high copy number of a specific transport proteins, VDAC (Voltage-Dependent Anion Channel), which can form pores on the membrane, becoming mostly permeable to ions and metabolites up to

5000 Da. However, the IMM is a highly selective membrane, thanks to the presence of cardiolipin, a specific phospholipid that makes the membrane permeable only to some ions. Despite the interest and the effort of many laboratories, for many years the problem of the molecular identity of the transport protein that allows Ca^{2+} to pass through the IMM was unsolved.

The mitochondrial Ca^{2+} uniporter

In 2008, thanks to the mass spectrometry analyses, Mootha and co-workers reported a mitochondrial "genoteque" called MitoCarta. It was obtained from highly purified and crude mitochondrial preparations, derived from 14 different mouse tissues, to discover genuine mitochondrial proteins, further validated by GFP tagging (Pagliarini et al., 2008). They took into account only the proteins localized in the IMM, expressed in the majority of mammalian tissues and with homologues in vertebrates and kinetoplastids, identifying finally a protein named "Mitochondrial Calcium Uptake 1" (MICU1). MICU1 possesses one transmembrane domain and two canonical EF-hands, essential for Ca^{2+}-sensing. MICU1 was thus recognized as a modulator of the Mitochondrial Calcium Uniporter (MCU) (Perocchi et al., 2010). The MitoCarta database and the molecular identification of MICU1 set the basis for the subsequent identification of MCU. In 2011 Rizzuto's and Mootha's laboratories identified a protein, encoded by the CCDC109A gene, which satisfies all the requirements of the bona fide Mitochondrial Calcium Uniporter (MCU) (Baughman et al., 2011; De Stefani et al., 2011).

The pore-forming subunits

MCU: mitochondrial calcium uniporter

In 2011, CCDC109A gene was recognized as the gene that encodes for the MCU. Indeed, MCU overexpression in HeLa cells strongly increases mitochondrial Ca^{2+} uptake while its silencing by siRNA drastically reduces it. Importantly, Baughman et al. demonstrated in vivo that knockdown of MCU in liver triggers complete inhibition of mitochondrial Ca^{2+} uptake in response to extra-mitochondrial pulses of Ca^{2+} (Baughman et al., 2011). De Stefani et al. demonstrated that MCU is necessary and sufficient to mediate mitochondrial Ca^{2+} uptake (De Stefani et al., 2011). Indeed, they showed that purified MCU formed a RuR-sensitive channel in planar lipid bilayers. MCU consists of two transmembrane domains across the IMM but it lacks classical Ca^{2+}-binding domains. The loop region that faces the intermembrane space (IMS), appears to be too small to contain regulatory elements. Blue native gel separation experiments of purified mitochondria showed a high-molecular-weight complex containing MCU with an apparent molecular weight of 480 kDa. Indeed, in the following years, several other proteins were identified (Figure 3). Several years later the firsts finding, four independent groups characterized the tetrameric architecture of the full-length Fungi homologs of MCU by Cryo-EM and/or X-ray diffraction approaches (Baradaran et al., 2018; Fan et al., 2018; Hirschi et al., 2017; Yoo et al., 2018). Of note, these Fungi MCU homologs share only about 40% of similarity with metazoan MCU, conserved in the transmembrane regions and in the coiled-coil domains, so Baradaran and coworkers performed Cryo-EM studies also on zebrafish MCU homolog, which displays the 91 % of similarity with human MCU. Although the resolution obtained is lower (8.5 Å), the overall structure is similar to that of Fungi MCU and also displays a tetrameric architecture (Baradaran et al., 2018).

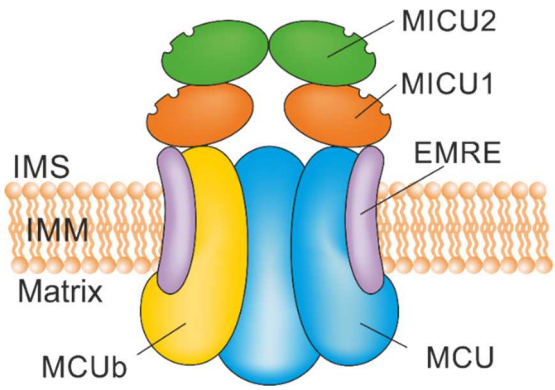

***Figure 4*: MCU complex: schematic representation of the mitochondrial calcium uniporter complex.** The pore-forming subunits comprise MCU, the MCU dominant negative isoform MCUb and EMRE. The regulatory subunits are composed MICU1 and MICU2.

MCUb: the dominant-negative of MCU

In 2013 Raffaello et al. identified CCDC109B gene that shares 50% homology with the MCU gene. The CCDC109B encoded protein is MCUb that has two predicted transmembrane domains, 50% sequence similarity with MCU but a different expression profile (Raffaello et al., 2013). Based on computational modelling, MCUb includes critical amino-acid substitutions in the pore region and therefore MCUb does not form a Ca^{2+}-permeable channel in planar lipid bilayers. In HeLa cells, MCUb is part of the MCU oligomer and exerts a dominant-negative effect, reducing the mitochondrial [Ca^{2+}] increase evoked by agonist stimulation (Raffaello et al., 2013).

EMRE: the essential MCU regulator

EMRE is a 10-kilodalton protein, with a single transmembrane domain and was identified in 2013. In its absence, uniporter channel activity is lost, despite intact MCU expression and oligomerization; thus, the name "Essential MCU Regulator" (EMRE). EMRE is required for the interaction of MCU with MICU1 and MICU2. Hence, EMRE is essential for uniporter current and regulates the calcium-sensing role of MICU1 and MICU2 on MCU conductance (Sancak et al., 2013).

The regulatory subunits

One of the main features of the mitochondrial calcium uptake is the sigmoidal response to the extra-mitochondrial calcium. At low cytosolic [Ca^{2+}], little Ca^{2+} enters through the channel while, upon cell stimulation, cytosolic [Ca^{2+}] increases, followed by rapid and efficient mitochondrial Ca^{2+} entry. These properties predicted by the presence of MCU regulators, including both negative modulators and activators.

MICU1: mitochondrial calcium uptake 1

Before the identification of MCU, targeted RNAi screen lead to the identification of MICU1 that showed an essential role in regulating agonist-induced mitochondrial Ca^{2+} uptake (Perocchi et al., 2010). Subsequent work revealed the complexity of MCU regulation and, in this context, the role of MICU1 was reassessed. Indeed, it was reported that MICU1 silencing increases basal mitochondrial [Ca^{2+}] causing mitochondrial Ca^{2+} overload and increased susceptibility to apoptotic stimuli. It was proposed that MICU1 sets the Ca^{2+} threshold of MCU activation, without affecting the kinetic properties of MCU-mediate Ca^{2+} uptake (Mallilankaraman et al., 2012). Further work confirmed the gatekeeping function that MICU1 exerts at low cytosolic [Ca^{2+}] but also demonstrated that MICU1 contributes to cooperative activation of mitochondrial Ca^{2+} uptake at high cytosolic [Ca^{2+}] demonstrating a dual role of MICU1 dependent on cytosolic Ca^{2+} calcium level (Csordás et al., 2013). Analysis of MICU1/MCU interaction established that MICU1 localizes in the inter membrane space and can form homo-oligomers (Csordás et al., 2013). Importantly, MICU1 possess two canonical EF hands domains facing the IMS, a helix-loop-helix structural domain present in calcium-binding proteins: upon Ca^{2+} binding, large conformational changes occur within one of the EF-hand domains present in the MICU1 sequence (Perocchi et al., 2010). Consequently, after Ca^{2+} binding, the formation of

multiple oligomers of MICU1 dimer occurs. The affinity of MICU1 for Ca^{2+} was calculated in the range of 15–20 μM. Thus, at resting cytosolic [Ca^{2+}], which is approximately 0.1 μM, MICU1 is free of Ca^{2+} and keeps the MCU channel closed. Upon cell stimulation, cytosolic [Ca^{2+}] rises and Ca^{2+} binds to MICU1, inducing MICU1 conformational changes and MCU activation (Mallilankaraman et al., 2012).

MICU2: the MCU gatekeeper

MICU2 is the paralog of MICU1 and was identified with another MCU regulator, MICU3 (Plovanich et al., 2013). Similar to MICU1, MICU2 possesses two highly conserved EF-domains. MICU2 silencing causes an increase in mitochondrial Ca^{2+} uptake while the overexpression causes a decrease upon agonist-induced Ca^{2+} uptake. The simultaneous silencing of MICU1 and MICU2 has an additive effect on mitochondrial Ca^{2+} uptake. Of note, MICU1 and MICU2 proteins level are dependent one to each other: in HeLa and HEK293T cell lines, MICU2 expression depends on the expression of MICU1 while the effect of MICU2 silencing on MICU1 seems to be cell-type dependent (Kamer and Mootha, 2014)

Patron et al. demonstrated that MICU1 and MICU2 form a heterodimer and play opposing effects on mitochondrial Ca^{2+} entry. In particular, MICU1 has a stimulatory role, while MICU2 inhibits Ca^{2+} uptake. Both are regulated by Ca^{2+} binding at their EF-hand domains. At low cytosolic [Ca^{2+}], the inhibitory role of MICU2 prevails, while at high cytosolic [Ca^{2+}] conformational modifications ensure prompt MICU1-dependent activation of mitochondrial Ca^{2+} uptake. Accordingly, a MICU2 mutant unable of binding calcium acts as gatekeeper even in high cytosolic [Ca^{2+}], while a MICU1 mutant loses the capability to cooperatively activate MCU (Patron et al., 2014)

MICU3

MICU3 doesn't show the ubiquitous tissues expression of MICU1 and MICU2 but it is expressed only in the CNS and, at low levels, in skeletal muscle. The MICU3 similarity with MICU1 and MICU2 is the mitochondrial targeting sequence (MTS) at the amino terminus and two canonical Ca^{2+}-binding EF-hand domains. It forms a disulfide bond-mediated dimer with MICU1, but not with MICU2, and it acts as an enhancer of MCU-dependent mitochondrial Ca^{2+} uptake, with no gatekeeping function (Patron et al., 2019). Of note, it was shown that neurons simultaneously express both MICU1-MICU2 and MICU1-MICU3 heterodimers: MICU1-MICU2 dimers avoid low vicious Ca^{2+} cycling in resting conditions while MICU1-MICU3 dimers allow organelle Ca^{2+} uptake even in the presence of small and rapid cytosolic Ca^{2+} signals. Thus, MICU3 in neurons allows enhancing MCU opening in order to guarantee organelle Ca^{2+} uptake also in response to small and fast increases of $[Ca^{2+}]$cyt (Patron et al., 2019).

Mitochondrial Ca^{2+} regulation of cellular energetics and cell death

The main physiological role of mitochondrial Ca^{2+} uptake is the control of the ATP production. The systems involved in this process are the tricarboxylic acid (TCA) cycle and the Mitochondrial Electron Transport Chain (mETC). Products from glycolysis and fatty acid metabolism are converted to acetyl-CoA which enters the TCA cycle, where it is fully oxidized to CO_2. More importantly, these enzymatic reactions generate NADH and FADH2 which provide reducing equivalents and trigger the electron transport chain (ETC). ETC consists of different protein complexes: complex I (NADH dehydrogenase), complex II (succinate dehydrogenase), complex III (ubiquinol cytochrome c reductase), complex IV (cytochrome c oxidase). Electrons are transferred from NADH and FADH2 to O_2 through these complexes in a stepwise fashion: as electrons move along the respiratory chain, energy is stored as an electrochemical H^+ gradient across the inner membrane, thus creating a negative mitochondrial membrane potential (estimated around -180 mV against the cytosol). Then, H^+ are forced to re-enter into the matrix mainly through the F1F0-ATP synthase, which couples this proton driving force to the phosphorylation of ADP into ATP, according to the chemiosmotic principle. ATP is then released to IMS through the Adenine Nucleotide Translocase (ANT), which exchanges ATP with ADP to provide a new substrate for ATP synthesis.

Within this mechanism, mitochondrial Ca^{2+} contributes by activating three enzymes of the TCA cycle, i.e. pyruvate-, α-ketoglutarate- and isocitrate-dehydrogenases with different mechanisms: pyruvate dehydrogenase is activated through a Ca^{2+}-dependent dephosphorylation step, the others via direct binding to a regulatory site (McCormack et al., 1990). Those three enzymes represent rate-limiting steps of the Krebs cycle thus controlling the feeding of electrons into the respiratory chain and the generation of the proton gradient across the inner membrane, necessary for ATP production.

Besides the role in cell life, mitochondrial Ca^{2+} plays an important role also in programmed cell death. Increase in $[Ca^{2+}]$cyt beyond a certain value sensitizes cells to apoptotic challenges, acting on the mitochondrial checkpoint. In fact, mitochondrial Ca^{2+} overload is a pro-apoptotic factor that could induce the swelling of mitochondria, with perturbation of the outer membrane, and in turn the release of mitochondrial pro-apoptotic factors into the cytosol (Giorgi et al., 2008).

Ca^{2+} binding to Cyclophilin-D positively regulates PTP opening (Basso et al., 2005). Once opened, PTP allows the release in the cytosol of intermembrane-residing apoptotic factors, such as cytochrome C, AIF (apoptosis-inducing factor) and Smac/DIABLO, which can trigger apoptosis by both a caspase-dependent and a caspase-independent pathway (Giorgi et al., 2012). Physiological mitochondrial $[Ca^{2+}]$ oscillations do not induce PTP opening, but become effective with the synergistic action of pro-apoptotic challenges (such as ceramide or staurosporine) (Pinton et al., 2001).

ROS and mitochondrial calcium signaling

Mitochondria are the primary site of ROS production, being the localization site of the respiratory chain. During mitochondrial respiration, 1–2% of molecular oxygen is converted into ROS, in particular from the complexes I and III (Murphy, 2009).

As discussed above, mitochondrial Ca^{2+} promotes ATP synthesis by activating enzymes of the Krebs cycle and it has been suggested that the increased metabolic rate and oxygen consumption in response to increases in mitochondrial calcium entry leads to an increase of the ROS levels (Brookes et al., 2004). Mitochondrial Ca^{2+} may promote mROS formation directly by stimulating mROS-generating enzymes such as glycerol phosphate and α-ketoglutarate dehydrogenase (Tretter and Adam-Vizi, 2004; Tretter et al., 2007). Indeed, physiological $[Ca^{2+}]$ stimulates the production of H_2O_2 associated with glycerol phosphate oxidation and probably

one of the crucial events is the stimulation of glycerol-3-phosphate deydrogenase by Ca^{2+} (Tretter et al., 2007). Moreover, Ca^{2+} is a regulator of the mitochondrial metabolism by activating dehydrogenases. Alpha-ketoglutarate dehydrogenase (α-KGDH) activation has been demonstrated by measuring the NADH formation by the isolated α-KGDH in the presence of different Ca^{2+} concentrations. Furthermore, the rate of H_2O_2 formation, measured in α-KGDH isolated enzyme, demonstrated a direct correlation between Ca^{2+} and H_2O_2 concentrations, whit or without the presence of NAD^+ (Tretter and Adam-Vizi, 2004)

Mitochondrial Ca^{2+} may promote mROS formation also indirectly, for example by activating nitric oxide synthase (NOS) that, by forming NO, inhibits complex IV activity, leading to excessive mROS formation (Görlach et al., 2015). So, Ca^{2+} stimulates the TCA cycle and thus enhances the electron flow through the respiratory chain and, at the same time, Ca^{2+} stimulates the nitric oxide synthase generating nitric oxide. The nitric oxide can, in turn, inhibit thecomplex IV. These events increase ROS generation during the cycle of the oxidation and reduction of the Coenzyme Q10 in the complex III of the respiratory chain. At the same time, Ca^{2+} and nitric oxide can enhance ROS by inhibiting complex I. Finally at high concentrations, Ca^{2+} dissociates cytochrome c from the inner membrane and triggers the PTP opening thus leading to the cytochrome c release (Brookes et al., 2004). So, at high mitochondrial calcium concentrations, the production of mROS could be toxic compromising mitochondrial bioenergetics and cell functions (Tomar et al., 2017).

Nevertheless, it was shown that the resultant ROS of the described events are capable of inhibiting prolyl hydroxylase (PHD), stabilizing HIF-1α even in normoxia condition. (Yang et al., 2016). This enhanced HIF-1 activity under normoxic conditions is described as pseudohypoxia (Guzy et al., 2008).

Importantly, it has been also shown that tumour cells desensitize the mPTP to increases of $[Ca^{2+}]$ and ROS, enhancing their resistance to death (Sabharwal and Schumacker, 2014).

Finally, mitochondrial alterations are involved in tumour metabolism. These alterations result in increased ROS generation and abnormal calcium handling leading to changes of the redox status of cancer cells and tolerance of high ROS levels as they potentiate cellular growth and motility (Sabharwal and Schumacker, 2014).

Cell migration: the role of calcium

Cell migration is a natural process, important for embryonic development, wound healing and immunity. The migration process involves three important steps: remodeling of cytoskeleton, triggering cell polarity, and modifying the direction of movement in response to gradients of environmental variations. The role of cytosolic Ca^{2+} in cell migration is well-known: oscillations of cytosolic Ca^{2+} induce actin remodeling through the activation of the small GTPases RhoA and Rac1, the calmodulin Ca^{2+}-dependent kinase MLCK phosphorylates the myosin light chain (MLC) to promote Actomyosin contractions, the calpains, a Ca^{2+}-dependent proteases, control the assembly the focal adhesions. These events promote the formation of protrusions of the cell membrane, followed by the establishment of new focal adhesions (FA) at the leading edge to anchor the cytoskeleton to the extracellular matrix (Xu and Chisholm, 2014). During migration, polarized cells exhibit a cytosolic Ca^{2+} gradient with low Ca^{2+} concentration at the leading edge ensured by increased activity of the pumps that extrude intracellular Ca^{2+} (Tsai et al.,2014). This strategic cellular response allows local pulses of intracellular Ca^{2+} changes. Indeed, localized microdomains of high Ca^{2+} concentrations are more active at the front of the migrating cells to promote local focal adhesion proteins disassembly.

The role of mitochondrial calcium in cell migration in less know to respect the cytosolic calcium, but recent evidence supports the involvement of mitochondrial calcium in this

process. Different in vivo models have highlighted physiological functions of MCU: a study on C. elegans showed that epidermal wounding triggers a mitochondrial Ca^{2+} wave and a local production of mtROS. In turn, the loss of the nematode orthologue of MCU (MCU-1) suppressed mitochondrial Ca^{2+} uptake and impaired wound healing. The study shows that the inhibition of the mitochondrial Ca^{2+} wave, by MCU knock-out, prevents cytoskeleton remodelling during the healing process (Xu and Chisholm, 2014). In 2013, a study on zebrafish early development showed a correlation between mitochondrial Ca^{2+} and migration (Prudent et al., 2013). In this study, the morpholino-dependent knockdown of MCU induced a decrease of the mitochondrial Ca^{2+} pool and an increase of cytosolic Ca^{2+} level leading to deregulation of cell directionality and a decrease in actin polymerization dynamics and consequent cell migration defects. In fact, Ca^{2+}-oscillations and Ca^{2+} waves have a fundamental role during zebrafish early development, and in particular during gastrulation.

MCU-complex in cancer progression

The molecular characterization of the MCU protein complex opened the intriguing chance of dissecting the role of mitochondrial Ca^{2+} in cancer. The lasts years have witnessed an explosion of studies devoted to the dissection of the correlations between MCU complex components expression, tumour progression, and prognosis.

It is well know that the mitochondrial Ca^{2+} overload sensitizes cells to apoptotic stimuli, so one of the first observation is that this could be a promising strategy to eliminate cancer cells, which would have otherwise escaped apoptotic death (Giorgi et al., 2012). In agreement with these data, evidence suggested that cancer cells reduce MCU activity to increase their survival: indeed, colon and prostate cancers overexpress a microRNA that confers resistance to apoptotic stimuli by targeting MCU (Marchi et al., 2013). In detail, miR-25 overexpression reduces mitochondrial Ca^{2+} uptake and sensitization to apoptotic stimuli, while expression of an antimiR against miR-25 had a deleterious effect on cells that were stressed with some apoptotic stimuli. Furthermore, Chakraborty et al. showed that the silencing of MICU1 in ovarian cancer cells resulted in Ca^{2+} overload in the mitochondria that in turn causes increased susceptibility upon cisplatin treatment (Chakraborty et al., 2017). In line with this two studies, Loubiere et al. proposed, in a prostate cancer study, that the antidiabetic drugs and metabolic disruptors metformin and phenformin induce ER stress, ER Ca^{2+} release, mitochondrial Ca^{2+} uptake, organelle swelling, and apoptosis. Of note, they showed an increase of MCU mRNA levels following metformin treatment and this mechanism was reversed by MCU inhibition (Loubiere et al., 2017). In head and neck squamous cell carcinoma, MICU1 expression correlates with the expression of EZH2, which is a negative prognostic factor. This study showed that the silencing of EZH2 decreases MICU1 expression in human oral cancer cell lines. Additionally, also the EZH2 inhibitor DZNep causes a decrease of MICU1 expression that leads to a decrease cell viability and trigger apoptosis in the SCC25 and Cal27 cell lines (Zhou et al., 2015).

Finally, in pancreatic cancer, MCU and MICU1 genes undergo loss of heterozygosity, although whether MCU and MICU1 are oncogenes or tumour suppressor genes still needs to be clarified (Long et al., 2015).

However, other works show that, at least in some settings, a reduction in mitochondrial Ca^{2+} entry reduces tumour progression and metastasis formation.

By gene expression analysis, Curry et al. found that MCU expression is enriched in estrogen receptor (ER)-negative and basal-like tumours (Curry et al., 2013), and hypothesized an MCU-dependent survival advantage. In MDA-MB-231 cell line MCU silencing sensitized cells to caspase-independent cell death, but had no effect on caspase-dependent death. On the contrary, caspase-independent death triggered by treatment with the Ca^{2+} ionophore ionomycin was potentiated by MCU knockdown, suggesting that MCU inhibition could in principle be viewed as a therapeutical strategy against TNBC (Curry et al., 2013).

On the same line, research based on BreastMark algorithm confirmed the importance of MCU in breast cancer, showing poorer prognosis associated with MCU overexpression and MICU1 downregulation while overexpression of MICU1 and MCUb, alone or in combination, correlates with better prognosis (Hall et al., 2014). However, MDA-MB-231 cells were insensitive to MCU and MICU1 silencing upon cytotoxic treatment (Hall et al., 2014).

In addition, when different breast cancer subtypes were compared, a higher expression of MCU was found in estrogen receptor-negative patient samples, especially in basal-like breast cancers compared to luminal A and B subtypes (Curry et al., 2013).

Tosatto et al. showed that MCU expression correlates with breast cancer progression while no changes were detected in MICU1 and MICU2 mRNA expression (Tosatto et al., 2016). Knockdown of MCU decreases NADH and ROS levels while increasing the NADPH/NADH ratio and significantly reducing transcription of HIF-1α and its target genes. Moreover, the role of MCU in TNBC progression was corroborated by *in vivo* experiments. Indeed, the injection

of the MCU knock-out MDA-MB-231 cells into the fat pad of immune-deficient SCID mice markedly delayed primary tumour formation. In addition, at equal primary tumour size, absence of MCU impaired lung and lymph node invasion (Tosatto et al., 2016).

Similar to breast cancer, in hepatocellular carcinoma (HCC) tissues, MCU is frequently upregulated, MICU1 is downregulated and no significant differences are observed in MICU2, MCUb, or EMRE expression (Ren et al., 2017). These data suggest that MCU overexpression and MICU1 downregulation may offer a survival advantage against some apoptotic pathways.

Less is known about the role of MICU2 in cancer. According to the Human Protein Atlas, MICU2 appears to be a marker of good prognosis in renal cancer [www.proteinatlas.org] while, according to The Cancer Genome Atlas, MICU2 is amplified in prostate and breast cancer and highly mutated in breast and stomach cancer [TCGA; www.cancergenome.nih.gov].

A recent study demonstrates the relation between MCU and one of the fundamental step on the cancer hallmarks: the escape from senescence. Indeed, MCU was identified, together with ITPR2 (a member of the IP3 receptor family), as a novel regulator of both replicative and oncogene-induced senescence (OIS). During OIS, ITPR2 activity triggers Ca^{2+} release from the ER, condition that causes a mitochondrial Ca^{2+} accumulation and consequent loss of membrane potential, increased ROS production and finally senescence (Wiel et al., 2014).

All these data demonstrate that the MCU complex plays a role that is tumour and tumour stage dependent or even tissue dependent.

AIM

Triple-Negative Breast Cancer (TNBC) is a clinically heterogeneous category of tumours that lack expression of estrogen, progesterone and HER2 receptors and recent discoveries show that mitochondrial Ca^{2+} signalling is involved in this pathology (Curry et al., 2013; Hall et al., 2014; Tosatto et al., 2016).

The highly selective ion channel that allows Ca^{2+} enter into the mitochondria is the mitochondrial Ca^{2+} uniporter (MCU). MCU complex is composed of pore forming subunits, i.e. MCU, the MCU dominant-negative isoform MCUb and EMRE; and of regulatory subunits that finely tune the mitochondrial Ca^{2+} uptake: MICU1, MICU2 and MICU3. Recent evidence shows that MCU expression directly correlates with breast tumour progression and MCU deletion inhibits tumour and metastasis formation *in vivo* (Tosatto et al., 2016).

In this thesis we aim to uncover the role of MICU1, MICU2 and of MCUb in TNBC progression.

For this purpose, we genetically modified MICU1 and MICU2 activity in order to decrease mitochondrial Ca^{2+} uptake. Alternatively, we overexpressed MCUb. Our results demonstrate that MICU1, MICU2 and MCUb are involved in TNBC growth and metastasis formation and represent potential molecular targets for pharmacological intervention in triple negative breast cancer.

RESULTS

MICU1 expression is reduced in breast tumour samples

Previous work in our laboratory uncovered the link between MCU and breast cancer progression (Tosatto et al., 2016). Data analysis relative to tumour size and regional lymph node infiltration demonstrated a significant correlation of MCU and MCUb mRNA expression levels with breast cancer stages. In detail, MCU expression increases with tumour progression, while the expression of MCUb, the dominant-negative channel isoform, decreases (Tosatto et al., 2016). Concerning MCU regulators, the Human Protein Atlas [www.proteinatlas.org] reports moderate to strong immunostaining of MICU1 in most malignant tissues, while for MICU2 weak to moderate immunostaining is detected. Moreover, The Cancer Genome Atlas [TCGA; www.cancergenome.nih.gov] shows that MICU1 amplifications are commonly identified in many cancers and both MICU1 and MICU2 are amplified in prostate and breast cancer (Vultur et al., 2018). However, based on the Breast Mark algorithm, Hall. et al. reported that a significantly poorer prognosis in breast cancer patients, is associated with MCU overexpression and MICU1 under expression (Hall et al., 2014). Thus, whether or not changes in the expression of MCU complex components are fundamental for breast cancer progression is not clear yet. In order to decipher the role of MCU regulators in mitochondrial Ca^{2+} signalling in breast cancer we studied the expression of MCU, MICU1 and MICU2 in 20 breast tumoural samples compared to 10 non-tumoural breast samples. Our analyses showed a trend towards upregulation of MCU. No significant difference was observed in MICU2 expression while, strikingly, MICU1 was significantly downregulated (Fig. 4). This result, in line with Hall et.al., is apparently in contrast with other databases data. However, the small sample size of our set or the different distribution of cancer subtypes and stages between our set and the databases should be taken into account.

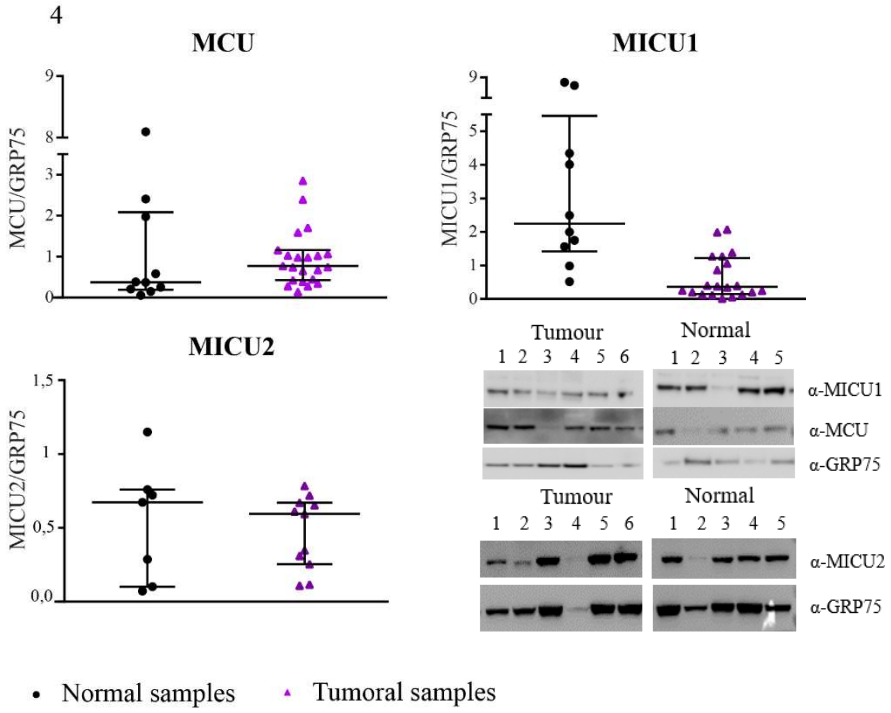

***Figure 4*: expression of MCU complex components is dysregulated in breast tumour samples.** Western blot analysis of MCU, MICU1 and MICU2 in 20 tumoural sample and 10 normal breast tissues. GRP75 was used as loading control. *p<0.05, two tailed, unpaired Mann Whitney test was performed. Data are presented as box-plot distribution.

To better understand the role of MICU1 in breast cancer progression, we silenced MICU1 in a triple negative breast cancer cell line (TNBC): the MDA-MB-231 cell line. As already reported for HeLa cells (Patron et al., 2014), short interfering RNA (siRNA)-mediated inhibition of MICU1 caused a significant increase in agonist-induced mitochondrial [Ca^{2+}] uptake. This is accompanied by a reduction of MICU2 expression indicating that, similarly to HeLa cells (Patron et al., 2014), in MDA-MB-231 cells, MICU1 is required for MICU2 stability (Fig. 5a-b). This data is in line with the permissive role of mitochondrial Ca^{2+} during breast cancer progression (Mammucari et al., 2018).

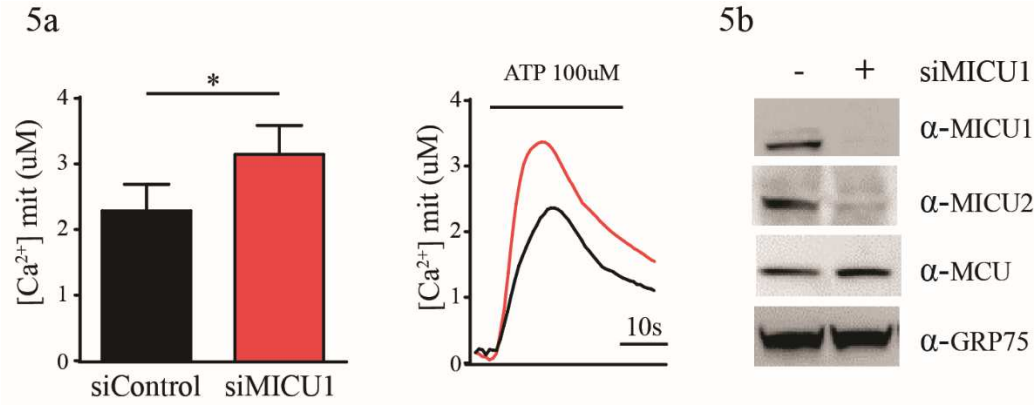

Figure 5: **MICU1 silencing increases mitochondrial[Ca^{2+}] uptake in MDA-MB-231 cells.**
a: cells were transfected with siMICU1 or siControl. 48h later mitochondrial [Ca^{2+}] uptake upon ATP stimulation was measured. (A two-tailed unpaired t-test was performed. n=3, *p< 0.05).
b: Western blot analysis of MCU, MICU1 and MICU2 in MDA-MB-231 cells. GRP75 was used as loading control.

MICU2 overexpression impairs MDA-MB-231 cell migration

To further explore the role of MCU regulatory subunits in MDA-MB-231 cell lines, we planned to genetically modulate their expression in order to decrease mitochondrial Ca^{2+} uptake. As reported above, genetic modulation of MICU1 does not represent a feasible approach, since both MICU1 overexpression and silencing increase mitochondrial Ca^{2+} uptake. Thus, we decided to transiently overexpress MICU2, the negative modulator of mitochondrial calcium entry. In line with results obtained in HeLa cells (Patron et al., 2014), overexpression of MICU2 in MDA-MB-231 cells reduced mitochondrial Ca^{2+} uptake (Fig.6a). In addition, in line with the permissive role of mitochondrial Ca^{2+} in cell migration (Tosatto et al., 2016), MICU2 overexpression triggered a decrease in cell migration (Fig.6b).

Nonetheless, transient MICU2 overexpression was achieved only in a relatively small portion of cells. Thus, to obtain higher protein expression and to perform long-term experiments, we decided to stably express MICU2 by infection of MDA-MB-231 cells with retroviral particles expressing MICU2. Once MDA-MB-231 cells had been infected and selected by puromycin treatment, we analyzed their mitochondrial Ca^{2+} transients, migration ability and clonogenic potential. MICU2 stable overexpression did not alter mitochondrial Ca^{2+} uptake neither in intact

nor in permeabilized cells (Fig. 6c-d). This unexpected effect was probably due to a low expression levels of exogenous FLAG-tagged MICU2 (Fig. 6e). We measured the agonist-induced cytosolic [Ca^{2+}] uptake and resting mitochondrial and cytosolic [Ca^{2+}] levels and we didn't find changes (data not shown).

In addition, the overexpression of MICU2 alone could result in yet uncharacterized rearrangements of the MCU regulatory complex. Indeed, MICU1 represents a limiting factor for the complex stability. It is reported that the MICU1-MICU2 dimer is the only endogenous available form of the regulatory complex but, while MICU1 is capable to form homodimers, MICU2 does not have this propriety (Patron et al., 2014).

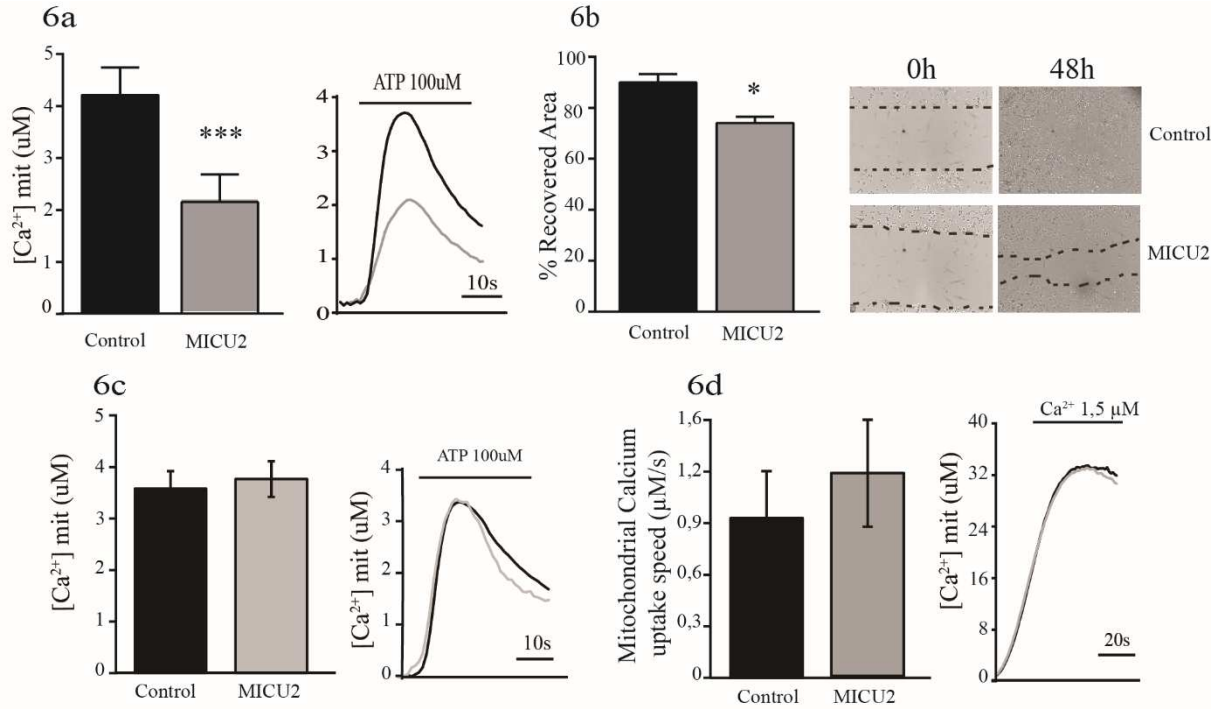

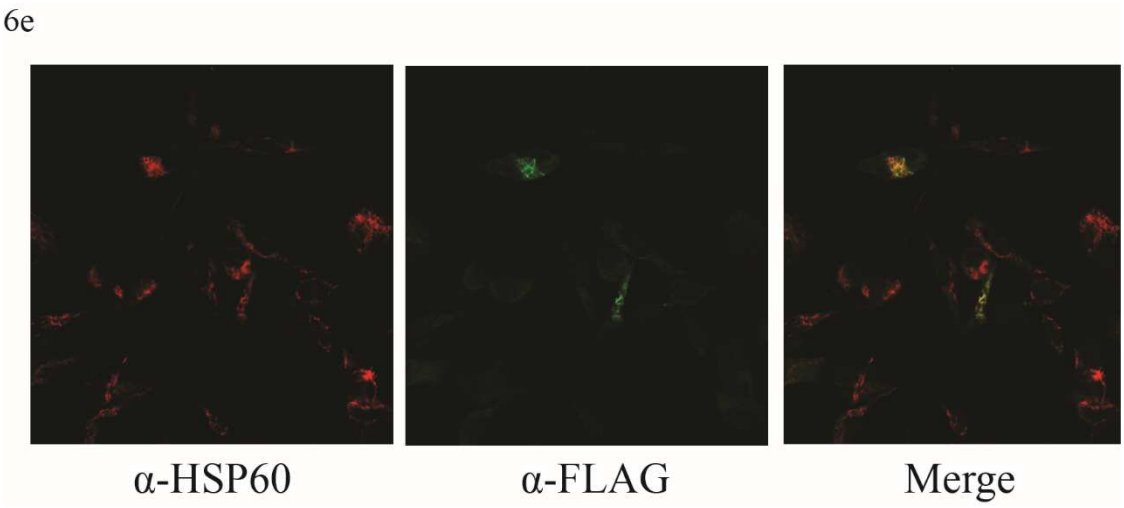

***Figure 6*: MICU2 overexpression impairs cell migration**
a: transient overexpression of MICU2 reduces mitochondrial [Ca^{2+}] uptake in MDA-MB-231 cells (*n=3*, ***p< 0.001).
b: transient overexpression of MICU2 impairs MDA-MB-231 cell migration. Cells were transfected with mock plasmids or plasmids expressing MICU2. The day after transfection a linear scratch was performed with a vertically held tip (time point 0h). Cell migration into the wounded area was monitored at 48-hour time point. The recovered area was measured and expressed as a percentage relative to 0-hour time point (*n=3,* *p<0.05).
c: mitochondrial **[**Ca^{2+}] measurements in control and MICU2 expressing MDA-MB-231 cells. mitochondrial [Ca^{2+}] uptake was measured upon ATP stimulation.
d: Measurements of Ca^{2+} uptake speed in control and MICU2- expressing MDA-MB-231 permeabilized cells, perfused with 1,5uM buffered [Ca^{2+}].
e: Immunofluorescence analysis shows the expression of MICU2-FLAG. Anti-FLAG antibodies were used to detect MICU2-FLAG and HSP60 was used as a mitochondrial marker.
Data information: in each panel, data are presented as mean ±SD. A two-tailed unpaired t-test was performed.

The overexpression of MICU1 and MICU2 EF-hand mutants impairs cell migration

The above results indicate that an alternative strategy to decrease the mitochondrial Ca^{2+} uptake should be seeked.

We took advantage of the intrinsic characteristics of MICU1 and MICU2. Indeed, MICU1 and MICU2 possess EF-hands domains that, upon Ca^{2+} binding, undergo large conformational changes. Mutations in these MICU1 and MICU2 regulatory domains cause a decrease in mitochondrial Ca^{2+} responses, indicating that Ca^{2+} itself controls the activity of the MCU regulatory complex (Patron et al., 2014). Thus, as a strategy to reduce agonist-induced mitochondrial [Ca^{2+}], we thought of expressing $MICU1^{EFmut}$ and $MICU2^{EFmut}$, alone or in combination in MDA-MB-231 cells (Fig.7a). The overexpression of $MICU1^{EFmut}$, of

MICU2^{EFmut} and of both caused a significant decrease in mitochondrial Ca^{2+} uptake (Fig.7b) and impaired cells migration (Fig.7c).

However, by transient transfection we were able to express the proteins of interest only in 50% of the cells. For this reason, we decided to produce stable cell lines, as reported hereafter.

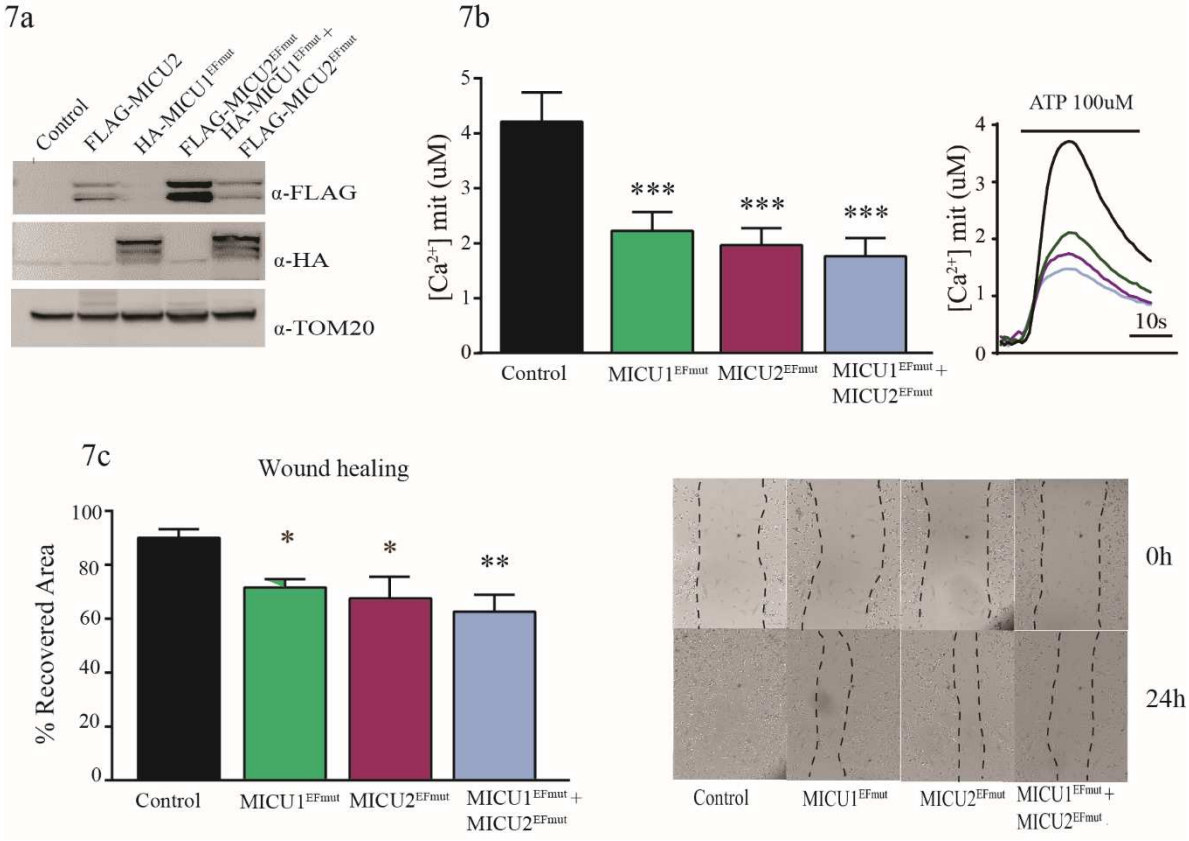

***Figure 7*: The transient overexpression of MICU1 and MICU2 EF-hand mutants impairs cell migration.**
a: Western blot analysis of FLAG-MICU2, HA-MICU1^{EFmut}, FLAG-MICU2^{EFmut}, HA-MICU1^{EFmut} + FLAG-MICU2^{EFmut} transfected MDA-MB-231 cells with αFlag and αHA antibodies. TOM20 was used as loading control.
b: Cells were transfected with mock plasmids or plasmids expressing MICU1^{EFmut}, MICU2^{EFmut}, MICU1^{EFmut} + MICU2^{EFmut}. 48h later mitochondrial [Ca^{2+}] uptake upon ATP stimulation was measured (*n=3*, ***p< 0.001).
c: Cells were transfected with mock plasmids or plasmids expressing MICU1^{EFmut}, MICU2^{EFmut} or MICU1^{EFmut} together with MICU2^{EFmut}.The day after transfection a linear scratch was performed with a vertically held tip (time point 0h). Cell migration into the wounded area was monitored at 48-hour time point. The recovered area was measured and expressed as a percentage relative to 0-hour time point (*n=3,* *p<0.05, **p<0.01).
Data information: in each panel, data are presented as mean ±SD. One Way Anova test was performed.

The stable expression of MICU1^{EFmut} and of MICU2^{EFmut} decreases mitochondrial Ca^{2+} uptake in permeabilized cells and impairs cell migration.

To obtain expression of the proteins of interest in most cells and to perform long-term experiments, we decided to stably express MICU1^{EFmut} and MICU2^{EFmut} by retroviral infection of MDA-MB-231 cells. Once MDA-MB-231 cells had been infected and selected by puromycin treatment, we analyzed mitochondrial Ca^{2+} transients, migration ability and clonogenic potential of the infected cells.

Surprisingly, stable expression of MICU1^{EFmut} or MICU2^{EFmut} did not reduce mitochondrial Ca^{2+} uptake upon ATP stimulation (fig. 8a-b). To better clarify whether mitochondrial Ca^{2+} entry is affected in these clones, we measured mitochondrial Ca^{2+} uptake speed in permeabilized cells. Mitochondrial Ca^{2+} uptake speed was decreased in MICU1^{EFmut} or MICU2^{EFmut} stably expressing cells, compared to the controls (fig.8c). Next, we evaluated resting and agonist-induced cytosolic [Ca^{2+}] and resting mitochondrial [Ca^{2+}] levels (fig. 8d-e-f). We measured an increase in cytosolic [Ca^{2+}] upon stimulation while resting mitochondrial and cytosolic [Ca^{2+}] levels were unchanged.

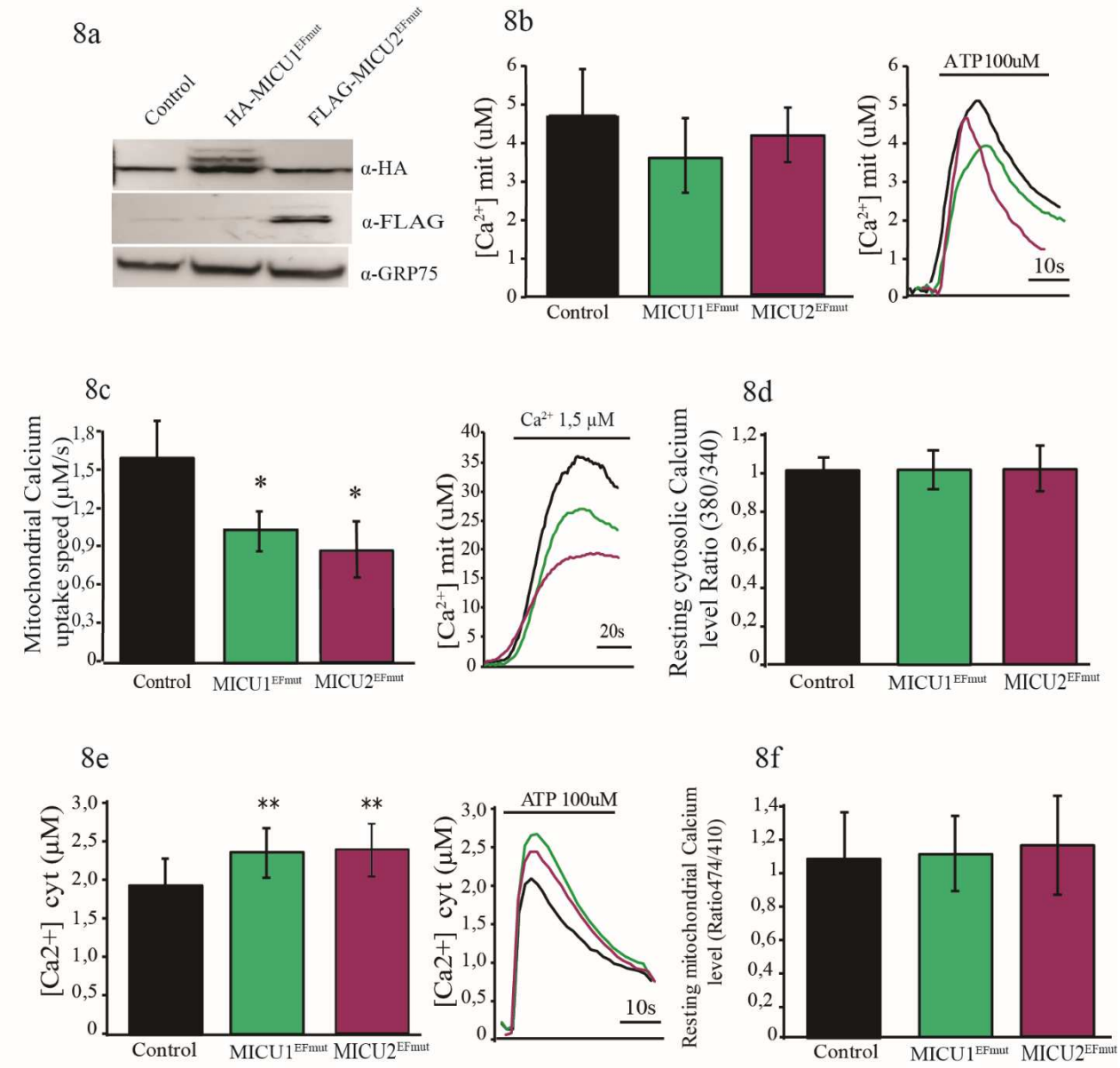

***Figure 8 (a-f)*: Both MICU1^{EFmut} and MICU2^{EFmut} stable expression decreases mitochondrial [Ca^{2+}] uptake in permeabilized cells**.

a: Western blot analysis of HA-MICU1^{EFmut} and FLAG-MICU2^{EFmut} overexpressing cells. MDA-MB-231 were infected with retroviral particles expressing HA-MICU1^{EFmut} and FLAG-MICU2^{EFmut} and western blotting analysis was performed with antibodies against Flag and HA tag.

b: mitochondrial [Ca^{2+}] measurements in control, MICU1^{EFmut} or MICU2 ^{EFmut} infected MDA-MB-231 intact cells. Mitochondrial [Ca^{2+}] uptake was measured upon ATP stimulation.

c: Measurements of Ca^{2+} uptake speed in control, MICU1^{EFmut}, MICU2 ^{EFmut} permeabilized MDA-MB-231 cells. (*n=3,* *p < 0.05).

d: MICU1^{EFmut} or MICU2^{EFmut} stable overexpression does not cause changes in resting cytosolic calcium levels evaluated through ratiometric imaging of the permeable fluorescent probe FURA-2AM.

e: Agonist-induced [Ca^{2+}]cyt transients are increased in MICU1^{EFmut} or MICU2 ^{EFmut} stable overexpressing cells upon ATP stimulation (*n=3***, p<0.01).

f: MICU1^{EFmut} or MICU2^{EFmut} stable overexpression does not cause changes in resting mitochondrial calcium levels evaluated through ratiometric imaging of the mitochondrial targeted 4mtGCaMP6f.

Data information: in each panel, data are presented as mean ±SD. One Way Anova test was performed.

We decided to study the migration capacity of MICU1^{EFmut} and MICU2^{EFmut} expressing cell lines by wound healing and we found a significant decrease in both conditions (fig.8g) while cell growth and colony formation didn't show any difference respect to the control (fig 8h-i).

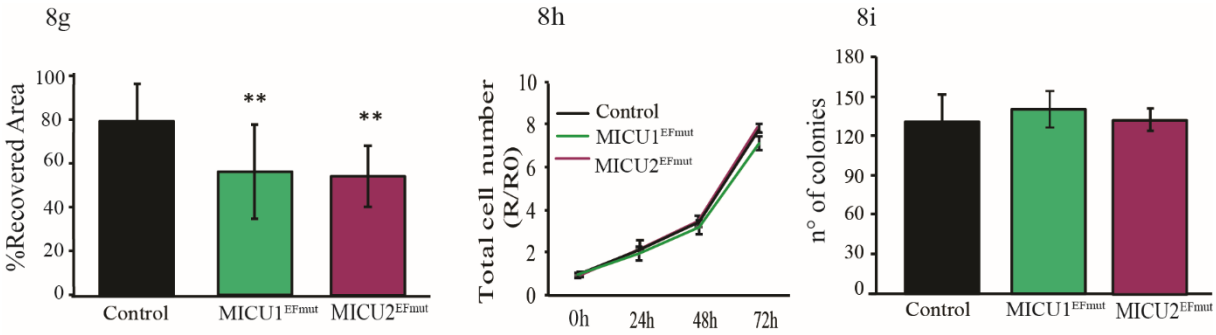

***Figure 8 (g-i)*: Both MICU1^{EFmut} and MICU2^{EFmut} stable expression impairs wound healing.**
g: MICU1^{EFmut} or MICU2^{EFmut} stable overexpression impairs MDA-MB-231 cell migration. 24 hours after cell plating, a linear scratch was performed with a vertically held tip (time point 0h). Cell migration into the wounded area was monitored at 48-hour time point. The recovered area was measured and expressed as a percentage relative to 0-hour time point ($n=3$** $p<0.01$).
h: Cell proliferation is unaffected by MICU1^{EFmut} and MICU2^{EFmut} stable overexpression. Cell number was counted every 24 h for 3 days. Results are expressed as ratio R/R0 where R0 is the number of cells at the time of plating (0-h time point).
i: MICU1^{EFmut} or MICU2^{EFmut} stable overexpression does not affect the clonogenic potential of MDA-MB-231 cells. Cells were plated at low confluence (2×10^3/well of a 6-well plate). After 8 days, the number of colonies was counted (minimum 30 cells/colony).
Data information: in each panel, data are presented as mean ±SD. One Way Anova test was performed.

The stable co-expression of MICU1^{EFmut} and MICU2^{EFmut} reduces mitochondrial Ca^{2+} uptake and impairs wound healing

Accordingly to the results reported in figure 7c, the co-expression of MICU1^{EFmut} and MICU2^{EFmut} effectively decreased cell migration. We decided to create a cell line that stably express MICU1^{EFmut} and MICU2^{EFmut} simultaneously and at equimolar levels. For this purpose, we took advantage of an expression system based on the P2A self-cleaving peptide that allows to generate two separate peptides within a single transcript. This system lead to relatively high levels of protein expression compared to other strategies for multi-gene co-expression. In addition, due to its small size, the P2A peptide bears a lower risk of interfering with the function

of co-expressed genes (Wang et al., 2015). Thus, the P2A peptide was cloned between MICU1^{EFmut} and MICU2^{EFmut}. During the translation process, the ribosome skips the synthesis of a peptide bond located at the C-terminus of the P2A element, leading to separation between the upstream peptide (MICU1^{EFmut}) and the peptide downstream (MICU2^{EFmut}).

Once MDA-MB-231 cells had been infected with viral particles and selected by puromycin treatment, we analyzed the protein expression of MICU1^{EFmut}-P2A-MICU2^{EFmut} [(M1-M2)^{EFmut}] (Fig.9a). The expression levels of (M1-M2)^{EFmut} were almost comparable to the ones of the single transgenes. Moreover, the expression of (M1-M2)^{EFmut} caused a significant decline in agonist-induced mitochondrial [Ca^{2+}] uptake both in intact and in permeabilized cells (Fig.9b-c) indicating that the coexpression of MICU1^{EFmut} and MICU2^{EFmut} is more efficient than the expression of the single mutants. Then we characterized the global Ca^{2+} signalling by measuring resting and agonist induced cytosolic Ca^{2+} and resting mitochondrial Ca^{2+} levels (Fig.9d-e-f). No differences were observed in these parameter.

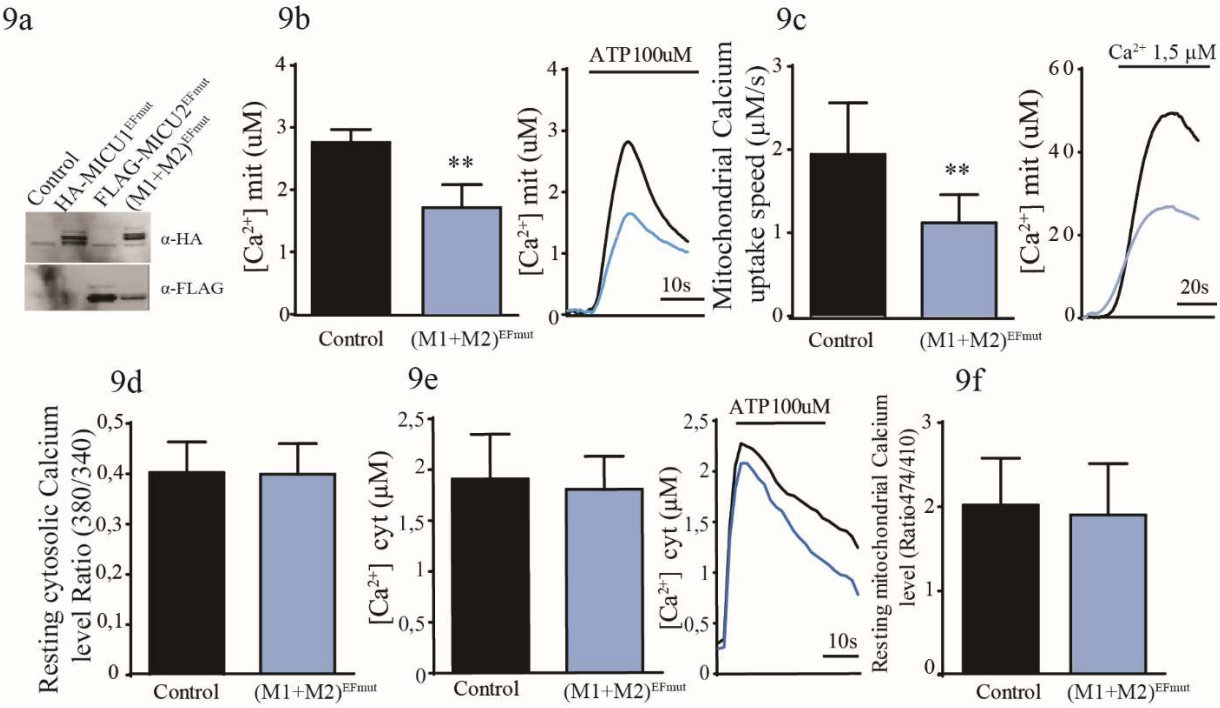

***Figure 9(a-f)*: The expression of (M1-M2)^{EFmut} decreases mitochondrial Ca^{2+} uptake.**
a**:** Western blot analysis of (M1-M2)^{EFmut} expression in MDA-MB-231 infected cells. HA antibodies were used to detect HA-MICU1^{EFmut} and FLAG antibodies to detect Flag-MICU2^{EFmut}.
b: [mitochondrial Ca^{2+}] measurements in control and (M1-M2)^{EFmut} infectedMDA-MB-231 cells, mitochondrial [Ca^{2+}] uptake was measured upon ATP stimulation (100uM) (*n=3,*** p<0.01).
c: Measurements of Ca^{2+} uptake speed in control and (M1-M2)^{EFmut} infected MDA-MB-231 permeabilized cells, perfused with 1,5uM buffered [Ca^{2+}] (*n=3,* ** p<0.01).
d: (M1-M2)^{EFmut} stable overexpression does not affect resting mitochondrial calcium levels evaluated through ratiometric imaging of the mitochondrial targeted 4mtGCaMP6f.
e: (M1-M2)^{EFmut} stable overexpression does not affect resting cytosolic calcium levels evaluated through ratiometric imaging of the permeable fluorescent probe FURA-2AM.
f: Agonist-induced [Ca^{2+}]cyt level is not altered in MICU1^{EFmut} or MICU2 ^{EFmut} stable overexpressing cells. [Ca^{2+}]cyt transient upon ATP stimulation was measured.
Data information: in each panel, data are presented as mean ±SD. A two-tailed unpaired t-test was performed.

As a consequence of reduced mitochondrial Ca^{2+} uptake, (M1-M2)^{EFmut} expression impaired TNBC cells motility, monitored by wound healing migration assay (Fig.6g). Importantly, proliferation of MDA-MB-231 cells was unaffected by (M1-M2)^{EFmut} expression (Fig. 9h). This data was confirmed also by the colony formation assay, in which the expression of (M1-M2)^{EFmut} did not inhibit cell growth (Fig.9i).

We next wanted to verify if mitochondrial Reactive Oxygen Species (mROS) act as molecular effectors of cell migration controlled by mitochondrial Ca^{2+} uptake. Indeed, mROS represent signalling molecules that translate mitochondrial inputs into different cell responses, including cancer cell migration and invasion.

Live cell imaging of the mitochondrial H_2O_2-sensitive HyPerRed probe (Ermakova et al., 2014) revealed that the simultaneous expression of MICU1^{EFmut} and MICU2^{EFmut} causes a reduction of mitochondrial H_2O_2 level (Fig.9j). This data suggest that ROS may represent signalling mediators of MICU1^{EFmut}P2AMICU2^{EFmut} regulated cell motility.

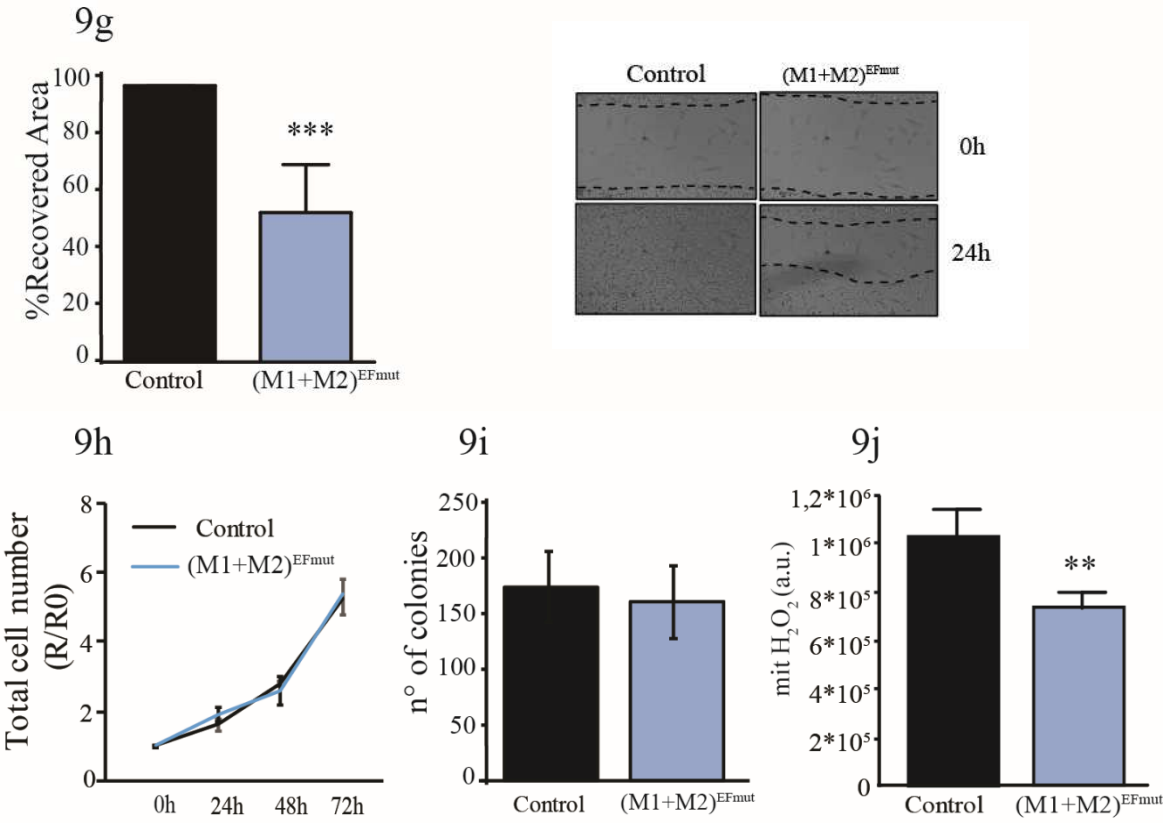

***Figure 9 (g-j)*: The expression of (M1-M2)^{EFmut} impairs wound healing.**
g: (M1-M2)^{EFmut} overexpression impairs MDA-MB-231 cell migration. The day after plating cells were scratched with a vertically held tip (time point 0h). Cell migration into the wounded area was monitored at 48-hour time point. The recovered area was measured and expressed as a percentage relative to 0-hour time point (*n=3****, p<0.005).
h: Cell proliferation is unaffected by (M1-M2)^{EFmut} stable overexpression. Cell number was counted every 24 h for 3 days. Results are expressed as ratio R/R0 where R0 is the number of cells at the time of plating (0-h time point).
i: (M1-M2)^{EFmut} stable overexpression does not affect the clonogenic potential of MDA-MB-231 cells. Cells were plated at low confluence (2×10^3/well of a 6-well plate). 8 days later, the number of colonies was counted (minimum 30 cells/colony).
j: Mitochondrial H_2O_2 levels significatively reduced after MICU1^{EFmut} and MICU2^{EFmut} overexpression. Cells were transfected with plasmids and HyPerRed probe (Fig.4e). 48 hours later production was measured. H_2O_2 was added as a positive control (*n=3***, p<0.01).
Data information: in each panel, data are presented as mean ±SD. A two-tailed unpaired t-test was performed.

A previous finding showed the correlation between the MCU expression and HIF1α activity (Tosatto et al., 2016). Indeed, it has been shown that MCU silencing caused a robust downregulation of HIF-1α protein both in normoxic and in hypoxic condition. Moreover, also the mitochondrial ROS depletion, by MitoTEMPO treatments, significantly blunted HIF-1α expression (Tosatto et al., 2016).

Since the decrease of mitochondrial calcium uptake by the overexpression of MICU1^{EFmut} and MICU2^{EFmut} cause a reduction of mitochondrial ROS production, we wished discover if this condition causes also the reduction of HIF1α expression. The overexpression of MICU1^{EFmut} and MICU2^{EFmut} causes a partial silencing of HIF1α suggesting that calcium *per se* or ROS regulate HIF1α expression.

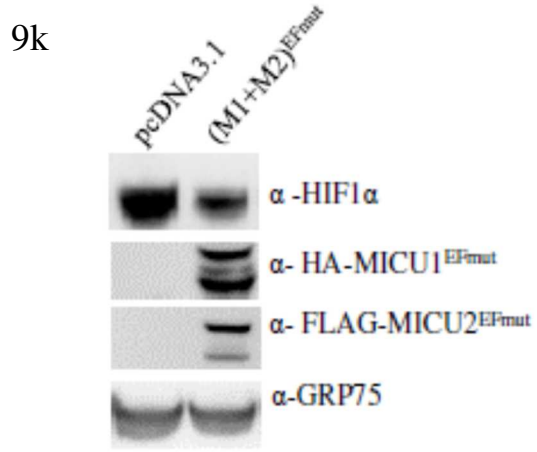

Fig. 9 (k): HIF1α levels are reduced after the overexpression of MICU1^{EFmut} + MICU2^{EFmut}
Cells were transfected with HA-MICU1^{EFmut} + FLAG-MICU2^{EFmut}. After 48 hours HIF-1α protein levels were measured by western blot. GRP75 was used as loading control.

The co-expression of MICU1^{EFmut} and MICU2^{EFmut} in MDA-MB-231 xenografts reduces metastasis formation *in vivo*

Next, we wanted to verify whether the co-expression of MICU1^{EFmut} and MICU2^{EFmut} alters the metastatic potential of MDA-MB-231 cells. To monitor *in vivo* tumour growth and metastasis formation, we took advantage of a luciferase detection system (see methods). Accordingly, we infected MDA-MB-231 cells expressing the luciferase gene with retroviral particles expressing (M1-M2)^{EFmut}.

Among the different generated clones, two (cl.8 and cl.12) were selected on the basis of their protein expression (Fig 10a) and tested for agonist-induced Ca^{2+} uptake (Fig.10b) and in vitro migration capability (Fig.10c).

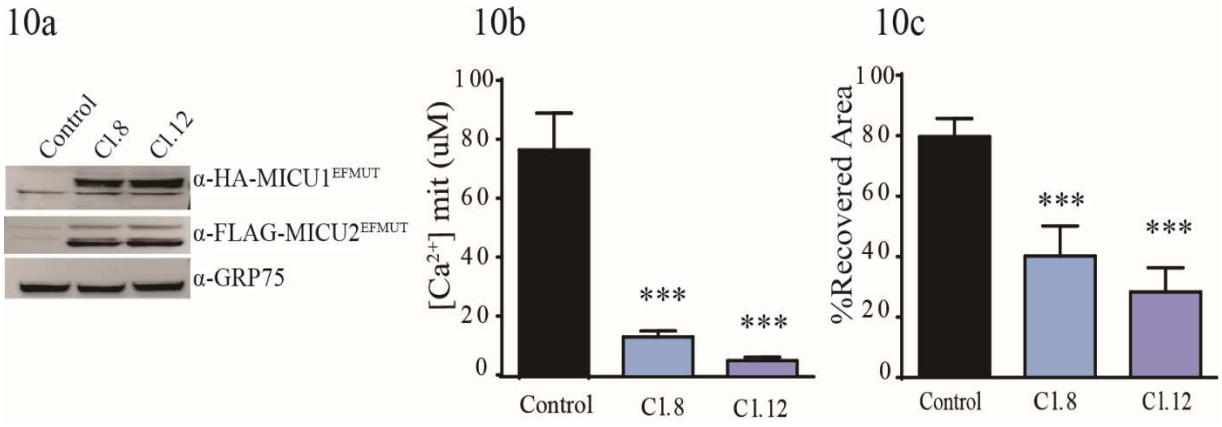

***Figure 10(a-c)*: Simultaneous expression of MICU1^{EFmut} and MICU2^{EFmut} in MDA-MB-231 stable clones reduces mitochondrial Ca^{2+} uptake and migration**

a:(M1-M2)^{EFmut} expression in MDA-MB-231 infected cells. HA antibodies were used to detect HA-MICU1^{EFmut} and FLAG antibodies to detect Flag-MICU2^{EFmut}. GRP75 was used as loading control.

b: mitochondrial [Ca^{2+}] measurements in control and (M1-M2)^{EFmut} clones carrying the firefly luciferase reporter gene. Mitochondrial [Ca^{2+}] uptake was measured upon ATP stimulation (One Way Anova, *n=3* ***p<0.005).

c:(M1-M2)^{EFmut} MDA-MB-231 clones carrying the firefly luciferase reporter have impaired migration ability in vitro. Cells were plated and the day after cells were scratched with a vertically held tip (time point 0h). Cell migration into the wounded area was monitored at 48-hour time point. The recovered area was measured and expressed as a percentage relative to 0-hour time point (One Way Anova, *n=3****p<0.005).

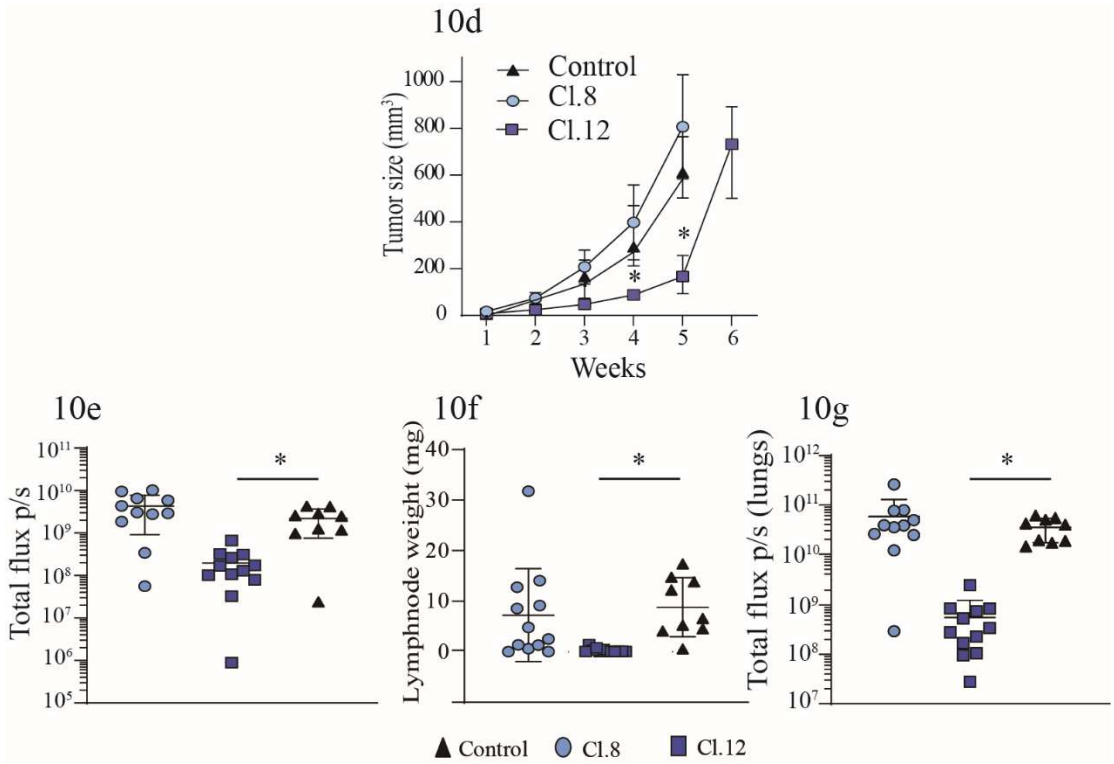

***Figure 10(d-g)*: Simultaneous expression of MICU1^{EFmut} and MICU2^{EFmut} in MDA-MB-231 cells xenografts reduces tumour formation and metastasis invasion in vivo.**

e: Total flux analysis of in vivo metastasis of lungs and lymph node area at the time of sacrifice.

f: Lymph nodes weight at the time of sacrifice.

g: Total flux analysis of explanted lungs at the time of sacrifice.

Data information: *p<0,05 *n* = 9 for Control, *n* = 11 for cl.8, *n* = 12 cl.12. One Way Anova test was performed.

The cells were then injected into the fat pad of SCID mice, and tumour size, lymph node infiltration, and metastasis formation were measured at different time points. The two clones gave two different results: indeed, the tumours formed in mice injected with cl.8 cells, had the same growth rate relative to the control, while tumour growth was slower in mice injected with cl.12 cells (Fig.10d). To compare the metastatic potential of tumours of equal size, control mice and mice injected with cl.8 cells were sacrificed at 5 weeks post-injection while mice injected with cl.12 were sacrificed at 6 weeks post-injection. We detected significant differences in the metastatic invasion of the lungs and lymph nodes area (Fig.10e), of lymph node weight (Fig.10f) and of lungs (Fig.10g) in cl. 12 injected mice compared to controls, while cl. 8 injected mice had the same rate of metastasis formation and lymph node invasion compared to controls (Fig.10e-f-g).

Due to the difference between the two clones, we decided to verify the maintenance of $MICU1^{EFmut}$ and of $MICU2^{EFmut}$ expression in the explanted tumours. Accordingly, we extracted proteins from the tumoural samples and we performed western blot analysis of $MICU1^{EFmut}$ and of $MICU2^{EFmut}$. Tumours derived from cl.12 conserved the expression of $MICU1^{EFmut}$ and of $MICU2^{EFmut}$ (Fig.10h) while tumours derived from cl.8 did not (Fig.10i), strongly indicating that the lack of impairment in tumour growth and metastasis formation of cl.8 was probably due to the loss of proteins expression.

10h

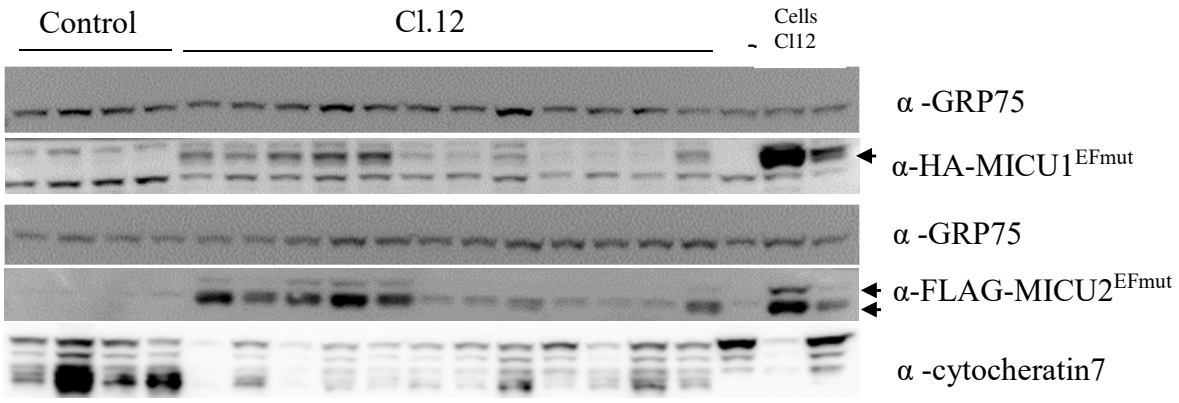

10i

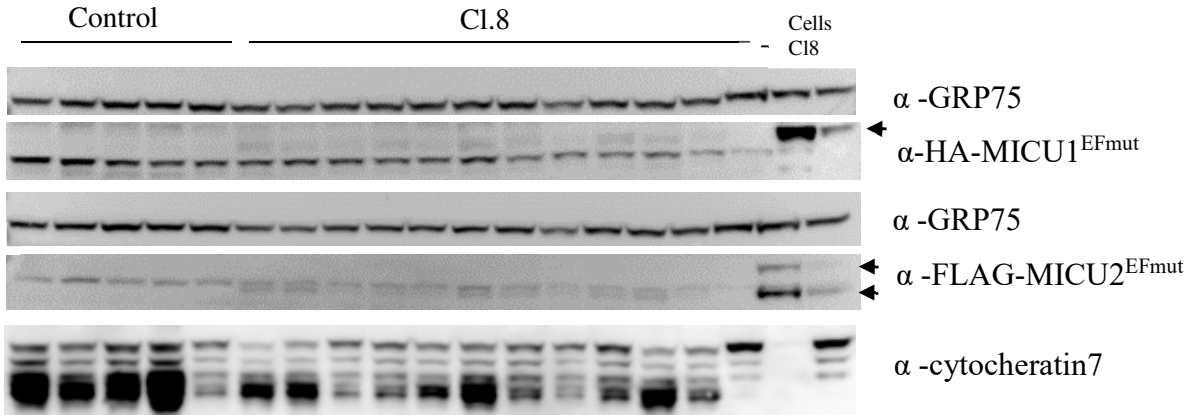

***Figure 10(h-i)*: Simultaneous expression of MICU1^{EFmut} and MICU2^{EFmut} in MDA-MB-231 cells xenografts reduces tumour formation and metastasis invasion in vivo.**
h-i: MICU1^{EFmut} and MICU2^{EFmut} expression in tumoural samples explanted from the mice. Antibodies against HA tag were used to detect MICU1^{EFmut} and antibodies against FLAG tag were used to detect MICU2^{EFmut}. Anti GRP75 was used as marker and anti cytokeratin7 was used as human specific marker.

MCUb expression correlates with breast tumour progression and cell migration

Data analysis relative to tumour size and lymph node infiltration demonstrated a significant decrease of MCUb expression with the increase in breast cancer clinical stages (Tosatto et al., 2016). Thus, we decided to better understand the role of MCUb in TNBC metastatic potential.

The overexpression of MCUb reduces mitochondrial calcium uptake in MDA-MB-231 cell line

We transiently overexpressed MCUb in MDA-MB-231 cell line (Fig.11a) to evaluate agonist-induced mitochondrial [Ca^{2+}] uptake. Similarly to other cell lines (Raffaello et al., 2013), in MDA-MB-231 cells the overexpression of MCUb causes a significant decrease in mitochondrial uptake (Fig.11b).

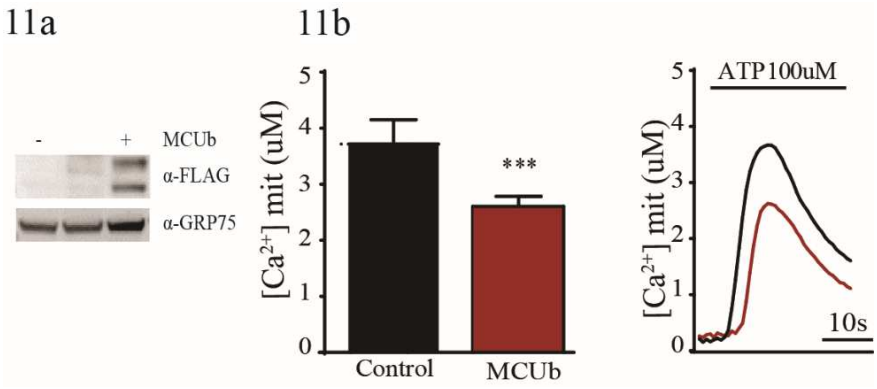

***Figure 11*(a-b): MCUb transient overexpression reduces mitochondrial Ca^{2+} uptake**
a: MCUb expression analysis. FLAG antibodies were used to detect FLAG-MCUb. GRP75 was used as loading control.
b: mitochondrial [Ca^{2+}] measurements in control and MCUb overexpressing cells. Mitochondrial [Ca^{2+}] uptake was measured upon ATP stimulation. (Two-tailed unpaired t-test *n=3*, ***p<0.005).

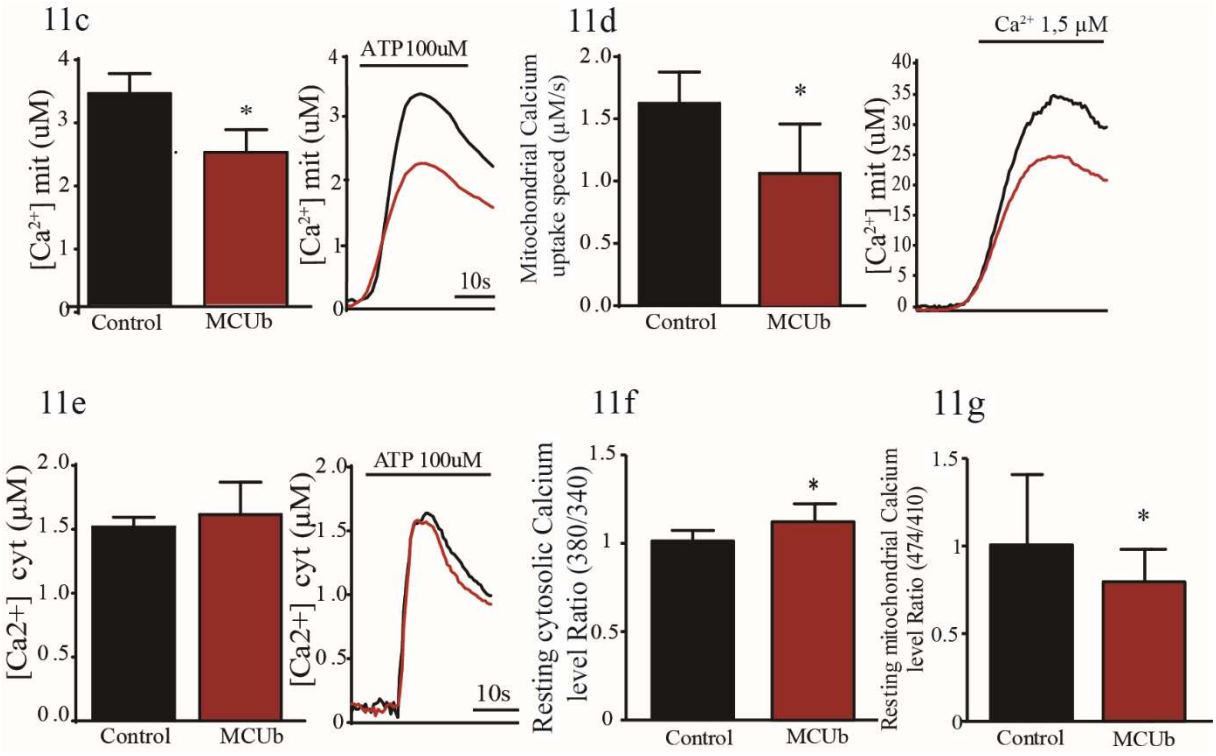

Figure 11(c-g): **MCUb stable overexpression reduces mitochondrial Ca^{2+} uptake.**
c: mitochondrial [Ca^{2+}] measurements in control cells and in MCUb stably overexpressing cells. Mitochondrial [Ca^{2+}] uptake was measured upon ATP stimulation. d: Measurements of Ca^{2+} uptake speed in control and MCUb infected MDA-MB-231 permeabilized cells, perfused with 1,5uM buffered [Ca^{2+}] (*n=3***, p<0.005). e: Agonist-induced [Ca^{2+}]cyt is unaltered in MCUb stable overexpressing cells. [Ca^{2+}]cyt transients upon ATP stimulation were measured. f: MCUb stable overexpression causes a significant increase in resting cytosolic Ca^{2+} levels evaluated through ratiometric imaging of the permeable fluorescent probe FURA-2AM(*p<0.05). g: MCUb stable overexpression causes a significant decrease in a resting mitochondrial Ca^{2+} levels levels evaluated through ratiometric imaging of the mitochondrial targeted 4mtGCaMP6f (*p<0.05).
Data information: in each panel, data are presented as mean ±SD. A two-tailed unpaired t-test was performed.

MCUb stable overexpression impairs cell growth, cell migration and colony formation

In order to increase the MCUb expression and with the perspective to perform *in vivo* experiments, we decided to stable overexpress MCUb in MDA-MB-231 cell line.

The stable overexpression of MCUb caused a significant reduction in agonist-induced mitochondrial [Ca^{2+}] uptake in intact and in permeabilized cells (Fig. 11c-d). We also verify the effect of MCUb expression on global cellular Ca^{2+} signalling. We measured mitochondrial resting [Ca^{2+}] levels and resting and agonist induced cytosolic [Ca^{2+}] levels. We didn't observe differences in cytosolic [Ca^{2+}] transient (Fig. 11e), while we found an increase in resting

cytosolic calcium levels (Fig.11) and a decrease in resting mitochondrial calcium levels (Fig.11g) indicating that MCUb overexpression impacts on global cellular Ca^{2+} signalling.

In line with the consistent effect on mitochondrial [Ca^{2+}] uptake, MCUb overexpression impaired cell motility, monitored by wound healing migration assay (Fig. 11h). Of note, cell proliferation was impaired by MCUb overexpression (Fig. 11i). This data was further confirmed by colony formation assay (Fig.11j).

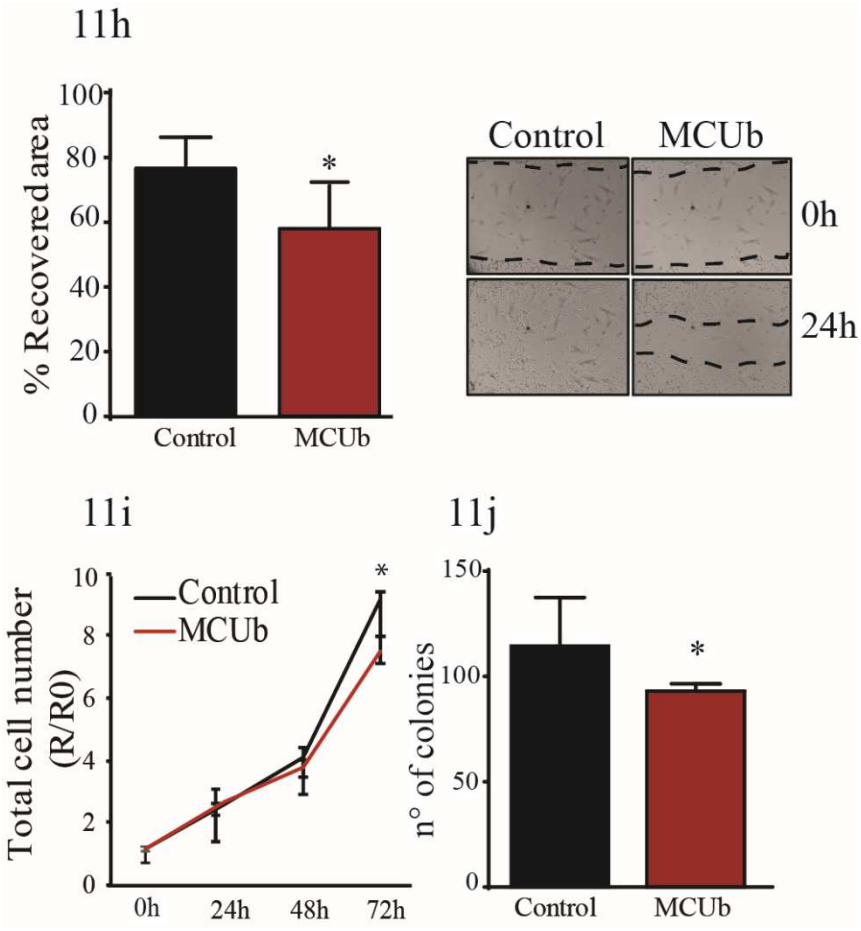

***Figure 11(h-j)*: MCUb stable overexpression impairs cell growth, migration and colony formation.**
h: MCUb overexpression impairs MDA-MB-231 cell migration. The day after plating cells were scratched with a vertically held tip (time point 0h). Cell migration into the wounded area was monitored at 48-hour time point. The recovered area was measured and expressed as a percentage relative to 0-hour time point(*$p<0.05$).
i: Cell proliferation is affected by MCUb stable overexpression. Cell number was counted every 24 h for 3 days. Results are expressed as ratio R/R0 where R0 is the number of cells at the time of plating (0-h time point) (*$p<0.05$).
j: MCUb overexpression reduces the clonogenic potential of MDA-MB-231 cells. Stable MCUb expressing and control cells were plated at low confluence (2×10^3/well of a 6-well plate). 7 days later, the number of colonies was counted (minimum 30 cells/colony) (*$p<0.05$).

Live cell imaging of the mitochondrial H_2O_2-sensitive HyPerRed probe (Ermakova et al., 2014) revealed that the expression of MCUb causes a reduction of mitochondrial H_2O_2 level (Fig.10k). At this point we wanted to verify if, as in the case of the mitochondrial calcium uptake decrease by the overexpression of $MICU1^{EFmut}$+ $MICU2^{EFmut}$, the expression of HIF1α undergo to an alteration. The overexpression of MCUb cause a decrease of HIF1α expression (Fig.11l)

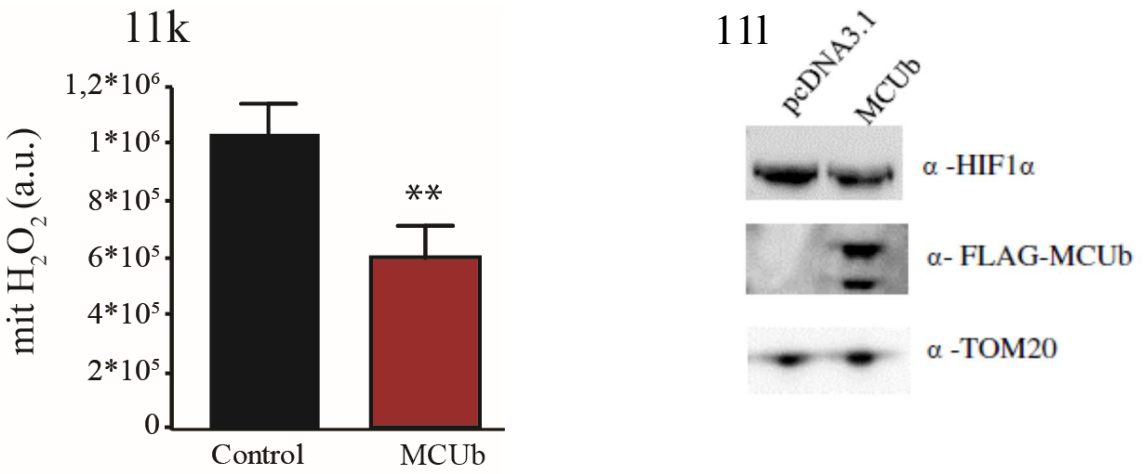

Figure 11(k-l): **MCUb overexpression alters mROS production and HIF1α expression**
k: Mitochondrial H_2O_2 levels are blunted after MCUb overexpression. Cells were transfected with MCUb and mitochondrial HyPerRed probe. 48 hours later H_2O_2 levels were measured. A two-tailed unpaired t-test was performed. n=3, *p< 0.05
l: Cells were transfected with FLAG-MCUb. After 48 hours HIF-1α protein levels were measured by western blot. TOM20 was used as loading control.

DISCUSSION

In recent years, the understanding of role of mitochondrial Ca^{2+} uptake has evolved in parallel to the definition of novel hallmarks of cancer, including the renewed interest for the deregulation of cellular energetics. Indeed, the molecular characterization of the Mitochondrial Calcium Uniporter (MCU) subunits (Mammucari et al., 2017) prompted the interest to explore new critical roles of Ca^{2+} uptake in cancer pathology.

It is well assessed that mitochondrial Ca^{2+} overload triggers apoptotic cell death (Giorgi et al., 2018). Thus, increased mitochondrial calcium entry has been considered as a promising strategy to eliminate aberrant cells, including cancer cells, which would have otherwise escaped apoptotic death. Indeed, a series of studies demonstrated that, at least in some settings, cancer cells negatively modulate MCU complex activity to increase their survival (Marchi et al., 2013; Chakraborty et al., 2017). However, the role of mitochondrial calcium homeostasis in cancer progression is more complex. Indeed, increased mitochondrial calcium uptake could also play a permissive role (Curry et al., 2013; Ren et al., 2017; Tosatto et al., 2016). It is important to note that the two extreme scenarios, i.e. increased apoptotic death or increased growth and metastatic potential in response to efficient mitochondrial Ca^{2+} uptake, are not mutually exclusive. Cancer cells continuously adapt and acquire pro-survival mechanisms during their progression, with the aim of developing an unrestrained proliferation. Thus, on one hand primary tumours need to inhibit mitochondrial Ca^{2+} loading in order to avoid any apoptotic stimuli sensitization. On the other hand, in metastatic cells, due to their peculiar characteristics, mitochondrial Ca^{2+} transients might have different favorable roles. The last years have witnessed an explosion of studies devoted to the dissection of the role of the mitochondrial calcium uniporter regulatory subunits in pathophysiology. Indeed, the MCU complex is a sophisticated machinery composed by the pore forming subunits, MCU, MCUb and EMRE,

and by the regulatory subunits, MICU1 and MICU2, involved in the finely tuning of MCU activity (Patron et al., 2014).

Within the heterodimer, MICU1 and MICU2 stimulate and inhibit MCU activity, respectively. Both MICU1 and MICU2 are regulated by Ca^{2+} through EF-hand domains. At low [Ca^{2+}], MICU2 plays a dominant effect and MCU activity is inhibited. At higher [Ca^{2+}], MICU1 exerts a stimulatory effect allowing the prompt response of mitochondria to cytosolic [Ca^{2+}] rises. Differently from MCU, MICU1 and MICU2 reside in the mitochondria inter-membrane space and are characterized by short half-life. Thus, in addition to MCU *per se*, the activity of the MICU1/MICU2 complex, which possibly is subject to fine-tuned modulation, could represent a potential pharmacological target in breast cancer.

An important indication of the role of MICU1 and MICU2 is suggested by a global evaluation of the mRNA expression of the pore-forming and modulatory subunits of the uniporter complex in breast cancer samples. MCU expression increases in parallel to tumour size and lymph node infiltration, while the expression of the heterodimer components MICU1 and MICU2 remains stable (Tosatto et al., 2016). Consequently, due to the relative defect in the gatekeeping mechanism (Patron et al., 2014), the prediction is that the mitCa^{2+} channel is constitutively open. In addition, based on the Breast Mark algorithm, Hall. et al. reported that a significantly poorer prognosis in breast cancer patients, is associated with MCU overexpression and MICU1 under expression (Hall et al., 2014).

These considerations highlight the necessity of a global examination and characterization of MCU complex components to deeply understand the role of the single subunits of the uniporter in the progression of the pathologies.

The role of mitochondrial calcium uptake in specific cancer settings has been extensively discussed. Nevertheless, the global examination of the MCU complex could shed light also on other diseases characterized by mitochondrial calcium dysregulation. In addition, the

identification of drugs or small molecules interfering with the activity of the MCU complex would facilitate the study of these pathologies and the development of therapeutic strategies.

As mentioned in the introduction, Wiel et al. discovered that MCU and ITPR2 are new senescence regulators. Indeed, they showed that the reduction of mitochondrial calcium uptake by MCU deletion allowed the cells to escape the oncogene-induced senescence (Wiel et al., 2014). In this case, an MCU complex activator could be helpful in order to avoid the senescence evasion. Another interesting study showed that MCU is involved in the pulmonary arterial hypertension (PAH), an obstructive vasculopathy characterized by excessive pulmonary artery smooth muscle cell (PASMC) proliferation, migration, and apoptosis resistance (tumour-like phenotype) (Hong et al., 2017). The striking result that they observed is that the indirect restoration of MCU (by miR-25 and miR-138 anti-miRs) reduces mitochondrial fission, restores glucose oxidation, reverses the Warburg effect, and decreases the pathologic rates of cell motility and migration and proliferation, data confirmed also *in vivo.* Thus, in this case, the loss of MCU is pathologic and the restoration of the MCU expression has therapeutic benefit.

Skeletal muscle activity is highly dependent on oxidative metabolism. Accordingly, skeletal muscle is the most affected tissue in constitutive MCU−/− mice (Pan et al., 2013). Moreover, MCU overexpression and downregulation trigger muscle hypertrophy and atrophy, respectively, both during postnatal development and in adulthood. Most importantly, MCU overexpression protects from denervation-induced muscle atrophy caused by sciatic nerve excision suggesting a possible therapeutic role of mitochondrial $Ca2^{+}$ uptake in muscle atrophy (Mammucari et al., 2015). Of note, a recent work analysed the MCU protein levels in human seniors subjected to muscle training showing an increased skeletal muscle MCU protein levels (Zampieri et al., 2016). This impressive result suggests that MCU represents a potential pharmacological target to counteract sarcopenia but also open an interesting field of study that

is the role of the MCU complex in cancer cachexia, where skeletal muscle metabolism and function plays a major role.

Moreover, a recent study showed the role of the mitochondrial calcium uniporter in fibrosis. MCU-mediated mitochondrial Ca^{2+} influx, and consequent increased ROS and ATP production, modulates macrophage activation to a profibrotic phenotype. In detail, the macrophages of MCU+/- mice showed attenuated profibrotic polarization after asbestos exposure together with a decrease in ATP production. In other words, the polarization of the macrophages to a profibrotic phenotype after exposure to asbestos is regulated by MCU-mediated ATP production. This profibrotic polarization was abrogated when the activity of MCU is inhibited and, of note, mice MCU-/- were protected from pulmonary fibrosis (Gu et al., 2017).These results indicate that MCU-targeting therapies could be helpful in the treatment of human fibrosis.

The data presented above indicate that therapeutic strategies should be different for different pathologies in which MCU is involved. Moreover, until now the detailed molecular mechanisms and the tissue specificity of the interaction of MCU with its regulatory subunits is not completely known. In addition, the transcriptional regulation and post-transcriptional modifications of the MCU complex represent a quite unexplored field and should be clarified. Finally, the long-term adaptation of cells to MCU complex manipulation is obscure and deserve further investigation.

In this thesis, we wished to validate the role of MCU complex components in triple negative breast cancer progression, both *in vitro* and in *in vivo*.

We started by studying the expression of MCU, MICU1 and MICU2 in breast tumoural samples and normal breast tumoural samples. We found a decrease in MICU1 expression in tumoural tissues compared to the normal tissues. The discrepancy with the TGCA database (Tosatto et

al., 2016) may be due the small sample size or the different distribution of cancer subtypes between our set and the databases. Thus, this issue deserves further investigation.

It is already reported that in HeLa cells, the silencing of MICU1 causes an increase in mitochondrial Ca^{2+} uptake, event caused by the contemporary loss of MICU2 (Patron et al., 2014). We verified that also in a triple negative breast cancer cell line (MDA-MB-231) the silencing of MICU1 triggers MICU2 loss and an increase in the mitochondrial Ca^{2+} uptake. This data is in line with the permissive role of mitochondrial Ca^{2+} uptake in tumour progression. However, it also indicates that the sole modulation of MICU1 expression is not a feasible strategy to reduce mitochondrial Ca^{2+} uptake. Thus, in order to decrease mitochondrial Ca^{2+} uptake, we overexpressed either MICU2 and or mutated isoforms of MICU1 and MICU2 in the EF-hands domains. The overexpression of MICU2, $MICU1^{EFmut}$ and $MICU2^{EFmut}$, alone or in combination causes a significant decrease in mitochondrial calcium uptake in MDA-MB-231 cell model reduced the migration potential of the cells. However, the stable overexpression of MICU2, $MICU1^{EFmut}$ and $MICU2^{EFmut}$ that we planned with the purpose to perform long lasting experiments, didn't reach the desired protein expression efficiently. This reflected on the mitochondrial calcium uptake: in the case of $MICU1^{EFmut}$ and $MICU2^{EFmut}$, even if we obtained a good reduction of mitochondrial calcium uptake in permeabilized cells, we were not able to achieved a significant decrease of mitochondrial Ca^{2+} uptake in intact cells. Intriguingly, we observed an increase in cytosolic Ca^{2+} transients meaning that the overexpression of $MICU1^{EFmut}$ and $MICU2^{EFmut}$ impinge on global Ca^{2+} homeostasis. Moreover, these conditions decreased the migration ability of the cells, indicating that even a mild effect on mitochondrial Ca^{2+} uptake may be sufficient,

Even worse, the stable overexpression of MICU2 was really inefficient and was not sufficient to decrease mitochondrial Ca^{2+} uptake: in HeLa cells (Patron et al., 2014), and we confirmed

this also in MDA-MB-231cells, the stability of MICU2 protein relies on the presence of MICU1.

Thus, we decided to optimized the strategy based on $MICU1^{EFmut}$ and $MICU2^{EFmut}$ overexpression. The stable, simultaneous and equimolar overexpression of $MICU1^{EFmut}$ and $MICU2^{EFmut}$, obtained by the P2A self-cleaving peptide strategy, caused the desired reduction of mitochondrial Ca^{2+} uptake, both in intact and in permeabilized cells. No differences were observed in cytosolic [Ca^{2+}] both at resting and agonist-induced conditions, and no differences was observed in resting mitochondrial [Ca^{2+}]. We monitored the capacity of those cells to migrate and recover a scratched area. The overexpression of $MICU1^{EFmut}$ P2A$MICU2^{EFmut}$ strongly reduced the migration potential without, affecting cell proliferation. We then performed an *in vivo* experiments to confirmed the *in vitro* data. One of the two clones selected for the *in vivo* experiments hampered tumour growth, lymph node invasion and metastasis formation. Unfortunately, the selected second clone lost the expression of $MICU1^{EFmut}$P2A$MICU2^{EFmut}$ during the tumoural progression. This fact highlighted one of the major difficulties that I found during the development of this work: indeed, the necessity of working with stable cell lines, with the purpose of the *in vivo* experiments, has collided with different cellular adaptations that in turn lead to a weak expression or loss of the proteins, or even in rearrangements in the systems that control the calcium homeostasis.

In the second part of the project, we extended our studies to the role of MCUb, the dominant negative isoform of MCU. While MCU expression increases with tumour progression, the expression of MCUb decreases (Tosatto et al., 2016). However, until now there are no studies that explore the role of MCUb in tumour progression. Here we found that the overexpression of MCUb impairs the migration of MDA-MB-231 cell line.

Furthermore, the stable overexpression of MCUb causes global rearrangement of Ca^{2+} homeostasis and a decrease, even if partial, in cell growth and in colony formation indicating a possible cytotoxic effect that needs to be verified.

Hereafter I summarize part of the results of my studies:

	MCUb		MICU2		MICU1EFMUT		MICU2EFMUT		$(M1\text{-}M2)^{EFmut}$	
	Transient	Stable	Transient	Stable	Transient	Stable	Transient	Stable	Transient	Stable
Mitochondrial $[Ca^{2+}]$transient	↓	↓	↓	=	↓	=	↓	=	↓	↓
Mitochondrial $[Ca^{2+}]$ basal		↓		=		=		=		=
Mit $[Ca^{2+}]$uptake speed		↓		=		↓		↓		↓
Cytosolic $[Ca^{2+}]$ transient		=		=		↑		↑		=
Cytosolic $[Ca^{2+}]$ basal		↑		=		=		=		=
Colony formation		↓		↓		=		=		=
Wound healing	↓	↓	↓	↓	↓	↓	↓	↓	↓	↓

One question is whether the different strategies to reduce mitochondrial calcium uptake in breast cancer trigger similar downstream events, involving the same effectors. MCU silencing reduced the production of mitochondrial Reactive Oxygen Species (mROS) (Tosatto et al., 2016) and these molecules are critical triggers of metastatic progression, both *in vitro* and *in vivo* (Porporato et al., 2014; Hempel and Trebak, 2017*).* In my thesis I showed that the reduction of mitochondrial Ca^{2+} uptake by the overexpression of $MICU1^{EFmut}$ and $MICU2^{Efmut}$ and by the overexpression of MCUb reduced mROS production and also HIF1α expression, indicating that different strategies to reduce mitochondrial calcium signalling, all impinge on mROS and HIF1α to hamper cancer progression. Thus, the final outcome of Ca^{2+} depletion signal appears to depend on alterations in the redox potential, which could in turn involve a large number of intracellular signalling cascades.

In the future, we plan to deeply investigate the signalling pathways involved in the regulation of the metastatic process by mitochondrial Calcium uptake. Mitochondrial Ca^{2+} plays a pivotal role in mitochondria activity thus impinging on the whole cell bioenergetics and metabolism. Indeed, even if cancer cells rely on glycolysis for ATP production even in normoxia conditions, mitochondria are still functional. In order to maintain their oxidative activity, a shift toward the use of substrates alternative to pyruvate, such as glutamate and fatty acids is often observed (Vyas et al., 2016). Moreover different intermediates of the TCA cycle are critical for the biosynthesis of different macromolecules, such as lipids, nucleotides and protein. The role of mitochondrial Ca^{2+} in such regulation is still obscure and deserves further investigation.

MATERIALS AND METHODS

Tissues collection from patients whit breast tumours

Tissue samples were obtained from the tissue biobank of clinical surgery 1 in the polyclinic Hospital of Padova. After the surgical operation, one tissue portion was immediately placed in liquid nitrogen and stored at -80°C until the subsequent analysis.

Cell culture

MDA-MB-231 cells were cultured in DMEM/F12 medium (1:1) (cat# 31331-028, Life technologies), supplemented with 10% FBS (Life technologies) with 1% Penicillin G - Streptomycin Sulfate (cat# ECB3001, Euroclone) and 1% L-Glutammine (cat# ECB3000D, Euroclone). Cells were maintained in culture at 37°C, with 5% CO2. A subcultivation ratio of 1:6 to 1:10 was guaranteed.

Transient transfections, infections and stable transductions.

SiRNA transfections:

Oligonucleotides (10 pmoles/cm2) were transfected using a standard Lipofectamine® RNAiMAX Transfection Reagent (cat# 13778-150, Life Technologies). To silence MICU1 was used an already publisched siRNA(Hall et al., 2014):

siRNA-MICU1:

Sense: CGAACUGAGCAAUAAGGAAUUUGdTdT

Antisense: AACAAAUUCCUUAUUGCUCAGUUCGCC

Plasmids overexpression

Proteins expression were obtained using a standard Lipofectamine® 2000 (cat# 11668019, Life Technologies). The plasmids expressing pcDNA3.1-MICU2-Flag, pcDNA3.1-

MICU1^{D233A,E244K,D423A,E434K}-HA (MICU1^{EFmut}), pcDNA3.1-MICU2^{D372A}-Flag (MICU2^{EFmut}), pcDNA3.1-MCUb-Flag and HyperRed were already available in our laboratory (Patron et al., 2014a; Raffaello et al., 2013; Tosatto et al., 2016).

Stable overexpression

MICU2-Flag, MICU1^{EFmut}-Flag, MICU2^{EFmut}-Flag, MCUb-Flag, MICU1^{EFmut}-HAP2AMICU2^{EFmut}-Flag stable overexpression was obtained by transducing MDA-MB-231 cells with retroviral vectors.

The coding sequences of the inserts MICU2-Flag, MICU1^{EFmut}-HA, MICU2^{EFmut}-Flag, MCUb-Flag were subcloned into BamHI and XhoI clonig sites of pBABE-puro cloning vector according to manifacturer's protocol (Addgene).

P2A self-cleaving cloning

To obtain MICU1^{EFmut}-HAP2AMICU2^{EFmut}-Flag was used a 2A self-cleaving peptide-based multi-gene expression system.

The DNA sequences coding for codon-optimized P2A peptides is

5’ ggttccggcgcaacaaacttctctctgctgaaacaagccggagatgtcgaagagaatcctggaccg 3’

MICU1^{EFmut}-HAP2A was cloned in the Zero Blunt® TOPO® PCR Cloning Kit using the following primers:

Primer forward

5’ gccggcgcca**cc**atgtttcgtcttaacacccttctg 3’

Primer reverse

5’ggatcccggtccaggattctcttcgacatctccggcttgtttcagcagagagaagtttgttgcgccggaacccagggaagcgtagtc aggcacatcgtaggggta3’

(Underlined restriction enzyme NAEI,BAMHI)

MICU1^{EFmut}-HAP2A was then subcloned in to NaeI, BamHI sites in pBABE-puro vector.

MICU2^{EFmut}-Flag was cloned into in the Zero Blunt® TOPO® PCR Cloning Kit using the following primers:

Primer forward

5': ggatccatggcggcggctgcgggaa

Primer reverse

5' gtcgacttacttatcgtcgtcatccttgtaatcgaaggggcccttgccggct

(Underlined restriction enzyme BamHI, SalI)

MICU2^{EFmut}-Flag was then subcloned in to BamHI, SalI sites in pBABE- MICU1^{EFmut}-HA-P2A vector.

Stable trasduction

We generated lentiviral particles from the simultaneous transfection of recombinant shuttle vector (pCMV-VSV-G Envelope) and pBABE-puro-MICU1^{EFmut}-HA-P2A-MICU2^{EFmut}-Flag in packaging HEK293GP (gag-pol) cells.

Adenovirus expressing mitochondrial mutated aequorin (AdCMVmAqMut) was constructed by Rutter et al. from plasmid mtAEQmut(Rizzuto et al., 1992) through the insertion of an EcoRI fragment into the multiple cloning site of pcDNA 3 (Invitrogen), and a correctly orientated *Kpn*I/*Xho*I fragment was inserted into vector pAdTrackCMV (Mitchell et al., 2001).

Plasmids

pBABE-puro (#1764) and pCMV-VSV-G (#8454) were obtained from Addgene.

mtGCaMP6f (Tosatto et al., 2016)

Western Blotting and Antibodies.

To monitor endogenous and overexpressed protein regulation, cells were lysated in RIPA-buffer (150 mM NaCl, 50 mM Tris, 1 mM EGTA, 1% Triton X-100, 0.1%SDS) and after 30'

of incubation on ice, 40 μg of total proteins were loaded, according to BCA quantification. Proteins were separated by SDS-PAGE electrophoresis, in commercial 4-12% acrylamide gels (Life technologies) and transferred onto nitrocellulose membranes (Life technologies) by wet electrophoretic transfer. Blots were blocked 1 hr at RT with 5% non-fat dry milk (BioRad) in TBS (0.5M Trizma –Sigma, 1.5M NaCl) solution (0.01% Tween) and incubated at 4°C with primary antibodies. Secondary antibodies were incubated 1 hr at RT. Washes after antibody incubations were done on an orbital shaker, three times for 10'each, with TBS-0,01% tween. We used the following antibodies: α-MCU (1:1000, Sigma), α-MICU1 (1:500, Novus), α – MICU2 (1:1000, Abcam), α-HA (1:2000 Cell Signaling), α-Flag(1:2000 Cell Signaling). Secondary, HRP-conjugated antibodies (1:5000) were purchased from BioRad. α – citocheratina 7 (1:1000 Cell Marque); anti-HIF1α (1:500, Becton Dickinson #610958)

Aequorin as a Ca^{2+} indicator

Aequorin is a 21 KDa photoprotein isolated from jellyfish *Aequorea Victoria* which emits blue light in the presence of Ca^{2+}. The aequorin originally purified from the jellyfish is a mixture of different isoforms called "heterogeneous aequorin" (Shimomura, 1986). In its active form the photoprotein includes an apoprotein and a covalently bound prosthetic group, called 75 coelenterazine. The apoprotein contains four helix-loop-helix "EF-hand" domains, three of which are Ca^{2+}-binding sites. These domains confer to the protein a particular globular structure forming the hydrophobic core cavity that accommodates the ligand coelenterazine. When Ca^{2+} ions bind to the three high affinity EF-hand sites, coelenterazine is oxidized to coelenteramide, with a concomitant release of CO2 and emission of light (Head et al., 2000). Although this reaction is irreversible, an active aequorin can be obtained *in vitro* by incubating the apoprotein with coelenterazine in the presence of oxygen and 2-mercaptoethanol. Reconstitution of an active aequorin (expressed recombinantly) can be obtained also in living cells by simple

addition of coelenterazine into the medium. Coelenterazine is highly hydrophobic and has been shown to permeate cell membranes of various cell types. Different coelenterazine analogues have been synthetized and are now commercially available.

The possibility of using aequorin as Ca^{2+} indicator is based on the existence of a well-characterized relationship between the rate of photon emission and the free [Ca^{2+}]. The first method used to correlate the amount of photons emitted to the free [Ca^{2+}] was that described by Allen and Blinks (Allen and Blinks, 1978). In the following years, this system was improved to achieve a simple algorithm that converts luminescence into [Ca^{2+}] values. Under physiological conditions of pH, temperature and ionic strength, this relationship is more than quadratic in the range of [Ca^{2+}] 10-5-10-7 M. The presence of 3 calcium binding sites in aequorin is responsible for the steep relationship between photon emission rate and free [Ca^{2+}] The [Ca^{2+}] can be calculated from the formula L/Lmax where L is the rate of photon emission at any instant during the experiment and Lmax is the maximal rate of photon emission at saturating [Ca^{2+}]. The rate of aequorin luminescence is independent of [Ca^{2+}] at very high (>10-4 M) and very low [Ca^{2+}] (< 10-7 M). However, as described below in more details, it is possible to expand the range of [Ca^{2+}] that can be monitored with aequorin. 76 Although aequorin luminescence is not influenced either by K+ or Mg^{2+} (which are the most abundant cations in the intracellular environment and thus the most likely source of interference under physiological settings) both ions are competitive inhibitors of Ca^{2+} activated luminescence.

pH was also shown to affect aequorin luminescence but at values below 7. Due to the characteristics described above, experiments with aequorin need to be done in well-controlled conditions of pH and ionic concentrations, notably of Mg^{2+}. Aequorin began to be widely used when the cDNA encoding the photoprotein was cloned, thus avoiding the purification of the native polypeptide and its microinjection. Moreover, the cloning of aequorin gene opened the way to recombinant expression and thus has largely expanded the applications of this tool for

investigating Ca^{2+} handling in living cells. In particular, recombinant aequorin can be expressed not only in the cytoplasm, but also in specific intracellular compartments by including specific targeting sequences in the engineered cDNAs (Hartl et al., 1989). Extensive manipulations of the N-terminal of aequorin have been shown not to alter the chemiluminescence properties of the photoprotein and its Ca^{2+} affinity. On the other hand, even marginal alterations of the C-terminal either abolish luminescence or drastically increase Ca^{2+} independent photon emission. For these reasons, all targeted aequorins synthesized in our laboratory include modifications of the photoprotein N-terminal.

The constructs used in our experiments are the wild-type and the mutated isoform of mitochondrial targeted aequorin (wtAEQmut and mtAEQmut) (Brini, 2008) and the isoform of cytosol targeted aequorin (CytAEQ)(Brini et al., 1995). The mitochondrial probes are obtained by fusing the initial 31 aminoacids of the subunit VIII of the human cytochrome c oxidase (COX) to the N-terminus of the photoprotein. The 31 COX aminoacids include the signal peptide and 6 aminoacids of the mature protein thus achieving the correct delivery of the aequorin to the matrix. The mtAEQ wild-type that permits [Ca^{2+}] measurements in a range of 10-15μM(Montero et al., 1995); the second is the mutated form of the mtAEQwt: the mtAEQmut. This probe has a point mutation in the second EF-domain (Asp119Ala) that cause a dramatic decrease in the Ca^{2+} affinity to the probe, thus permitting Ca^{2+} measurements in a range of 10-500 μM (Rizzuto et al., 1992). The CytAEQ is the wild-type isoform of the photoprotein. In, fact cells transfected with wtAEQ shows the expression of the photoprotein exclusively in the cytosol compartment. Indeed, the sequence of this aequorin is only modify at the 5' end of the coding region by adding the HA1 epitope tag(Brini et al., 1995)

Luminescence detection.

The aequorin detection system is derived from that described by Cobbold and Lee (Cobbold and Bourne, 1984) and is based on the use of a low noise photomultiplier placed in close proximity (2-3 mm) with aequorin expressing cells. Cells are seeded on 13-mm coverslips and put into a perfusion chamber. The volume of the chamber is kept to a minimum (about 200 µl). Cells are continuously perfused via peristaltic pump with KRB saline solution, thermostated via a water bath at 37°C.

The photomultiplier (Hamamatsu H7301) is kept into a dark box. The output of the amplifier-discriminator is captured by C8855-01-photoncounting board in an IBM compatible microcomputer and stored for further analysis.

Experimental procedures for Ca^{2+} measurments.

Ca^{2+} uptake in intact cells: cells were seeded onto 13 mm glass coverslips and allowed to grow to 50% confluence. The day before measuring, cells were transfected mtAEQwt, mtAEQmut or cytAEQ plasmids together with the indicated siRNA or plasmid.

The following day, coverslips with cells were incubated with 5 µM coelenterazine for 2 hours in KRB saline supplemented with 1mM CaCl2, and then transferred to the perfusion chamber. All aequorin measurements were carried out in KRB saline solution. Agonists were added to the same solution. The agonist stimulus used for maximal stimulation was 100 µM ATP.

The experiments were terminated by lysing cells with 100 µM digitonin in a hypotonic Ca^{2+}-rich solution (10 mM CaCl2 in H2O), thus discharging the unbound aequorin pool. The light signal was collected and calibrated into free $[Ca^{2+}]$ values by an algorithm based on the Ca^{2+} response curve of aequorin at physiological conditions of pH, $[Mg^{2+}]$ and ionic strength, as previously described.

Mitochondrial Ca^{2+} uptake in permeabilized cells: this experiment allows evaluating the characteristic of mitochondrial Ca^{2+} uptake machinery independent to ER Ca^{2+} release and the formation of microdomains of high [Ca^{2+}] in close proximity to mitochondrial Ca^{2+} channel. Cells were transfected with the mtAEQ mutated construct, using Lipofectamine 2000. After 24 hours of transfection, 2 hours before the experiment, we reconstituted the protein by adding the prosthetic group, coelenterazine WT.

Measurement in digitonin-permeabilized cells is performed perfusing cells in Intracellular Buffer (IB: KCl 130mM, NaCl 100mM, K2PO4 20mM, Hepes 200mM, Succinic Acid 50mM, Malic Acid 10mM, Pyruvate 10mM, MgCl2 10mM, pH 7.0 with KOH) for 60 seconds. Cells are then perfused with the same buffer with 20uM digitonin for 60 second and washed with IB buffer for other 60 second. Then we perfused a known [Ca^{2+}] solution, specifically containing 2mM CaCl2. In this way it possible evaluate the Ca^{2+} peak and its kinetic

Mitochondrial targeted mtGCaMP6f measurements

For measurements of resting mitochondrial [Ca^{2+}], cells were grown on 24-mm coverslips and transfected with plasmids encoding 4mtGCaMP6f. After 24 h, coverslips were placed in 1 ml of KRB and imaging was performed on a Zeiss Axiovert 200 microscope equipped with a 40×/1.4 N.A. PlanFluar objective. Excitation was performed with a DeltaRAM V high-speed monochromator (Photon Technology International) equipped with a 75 W xenon arc lamp. Images were captured with a high-sensitivity Evolve 512 Delta EMCCD (Photometrics). The system is controlled by MetaFluor 7.5 (Molecular Devices) and was assembled by Crisel Instruments. In order to perform quantitative. measurements, we took advantage of the isosbestic point in theGCaMP6f excitation spectrum: we experimentally determined in living cells that exciting GCaMP6f at 410 nm leads to fluorescence emission, which is not Ca^{2+} dependent. As a consequence, the ratio between 474-nm and 410-nm excitation wavelengths is proportional to [Ca^{2+}] while independent of probe expression (Hill et al, 2014). Cells were thus

alternatively illuminated at 474 and 410 nm, and fluorescence was collected through a 515/30-nm band-pass filter (Semrock). Exposure time was set to 200 ms at 474 nm and to 400 ms at 410 nm, in order to account for the low quantum yield at the latter wavelength. At least 15 fields were collected per coverslip, and each field was acquired for 10 s (1 frame/s). Analysis was performed with the Fiji distribution of ImageJ (Schindelin et al., 2012). Both images were background corrected frame by frame by subtracting mean pixel values of a cell-free region of interest. Data are presented as the mean of the averaged ratio of all time points.

Resting Cytosolic Ca^{2+} measurements

For the measurements of resting cytosolic [Ca^{2+}] cells were grown on 24-mm. After 24 hours cells were loaded with 2 μM Fura-2/AM (Thermo Fisher Scientific) diluted in Krebs-Ringer modified buffer (135 mM NaCl, 5 mM KCl, 1 mM MgCl2, 20 mM HEPES, 1 mM MgSO4,0.4 mM KH2PO4, 1 mM CaCl2, 5.5 mM glucose, pH 7.4) containing 0.02% pluronic acid. After 20 minutes at 37° the coverslips are washed with Krebs-Ringer modified buffer and imaging was performed on a Zeiss Axiovert 200 microscope equipped with a 40×/1.4 N.A. PlanFluar objective. 100uM ATP was added to elicit Ca^{2+} release from intracellular stores in order to control the saturation of the probe. Excitation was performed with a DeltaRAM V high-speed monochromator (Photon Technology International) equipped with a 75 W xenon arc lamp. Images were captured with a high-sensitivity Evolve 512 Delta EMCCD (Photometrics). The system is controlled by MetaMorph 7.5 (Molecular Devices) and was assembled by Crisel Instruments. Images were collected by alternatively exciting the fluorophore at 340 and 380 nm and fluorescence emission recorded through a 515/30 nm band-pass filter (Semrock). Exposure time was set to 50 ms. Acquisition was performed at binning 1 with 200 of EM gain. Image analysis was performed with Fiji distribution of the ImageJ software. Images were background

subtracted. Changes in fluorescence (340/380 nm ratio) was expressed as R/R0, where R is the ratio at time t and R0 is the ratio at the beginning of the experiment.

ROS production measurements

To determine mitochondrial hydrogen peroxide levels, cells were transfected with HyperRed plasmid (Ermakova et al., 2014), together with pcDNA3.1-MCUb plasmid and pcDNA3.1-MICU1^{EFmut} + pcDNA3.1-MICU2^{EFmut}.

Cells were imaged in Ringer's buffer solution 48 hours following plasmids transfection, using Cell Observer High Speed (Zeiss) microscope equipped with 40x oil Fluar (N.A. 1.3) or 100x oil alpha Plan-Fluar (N.A. 1.45) objective, CFP (Semrock HC) and YFP (Zeiss 46HE) single band filters, 420 and 505 nm LED's (Colibri, Zeiss) and an Evolve 512 EMCCD camera (Photometrics). Maximal mROS production was induced with 10 mM H2O2 as a positive control. HyperRed fluorescence was analized by ImageJ software. Statistical significance was determined using two-sided unpaired student's t-test.

Wound healing migration assay

For wound healing assays, cells were seeded and transfected at low confluency (30%) in 6-well plates, in complete medium. After 8 hours, cells were starved in medium without serum, for 24 hours. The day after, cell monolayers were scraped with a P200 tip, vertically held, to obtain a wound in each well; the medium was replaced with fresh one. Picture of migrating cells were taken at the indicated time point (time 0 as reference). A free software tool called "TScratch" (www.chaton.ethz.ch/software) was used for automated images analysis.

Clonogenic assay

To evaluate clonogenic potential, cells were counted (Scepter™ 2.0 Cell Counter) and seeded at very low density (10^3/well) into 6-well plates. After 8 days colonies were counted. Only colonies made of ≥ 30 cells were included in the quantification.

In vivo tumour assays

One control and two $(M1\text{-}M2)^{EFmut}$ clones were transduced with a retroviral vector coding for the Firefly Luciferase reporter gene(Breckpot et al., 2003). For orthotopic tumour assay, 10^6 cells were resuspended in 100ul DMEM and injected in the fat pad of six-week-old female SCID mice (Charles River Laboratories). The volume of tumour mass was measured by calipering at specific time points. In vivo imaging was performed at the day of sacrifice (5weeks post-injection for control, five weeks p.i. for $(M1\text{-}M2)^{EFmut}$ clone 8, and six weeks p.i. for $(M1\text{-}M2)^{EFmut}$ cl 12). D-Luciferin (Biosynth AG) (150 mg/kg) was injected i.p. to anesthetized animals. The light emitted from the bioluminescent tumours or metastasis was detected using a cooled charge-coupled device camera mounted on a light-tight specimen box (IVIS Lumina II Imaging System; Caliper Life Sciences). Regions of interest from displayed images were identified around metastatic regions, such as lymph nodes and lungs, and were quantified as total photon counts or photon/s using Living Image_ software (Xenogen). In some experiments, the lower portion of each animal was shielded before reimaging in order to minimize the bioluminescence from primary tumour. For ex vivo imaging, D-Luciferin (150 mg/kg) was injected i.p. immediately before necropsy. The lungs were excised, placed in a Petri plate, and imaged for 5 min. Animals were randomized before experiments, and no blinding was done.

BIBLIOGRAPHY

Allen, D.G., and Blinks, J.R. (1978). Calcium transients in aequorin-injected frog cardiac muscle. Nature *273*, 509–513.

Aspuria, P.-J.P., Lunt, S.Y., Väremo, L., Vergnes, L., Gozo, M., Beach, J.A., Salumbides, B., Reue, K., Wiedemeyer, W.R., Nielsen, J., et al. (2014). Succinate dehydrogenase inhibition leads to epithelial-mesenchymal transition and reprogrammed carbon metabolism. Cancer Metab. *2*, 21.

Baradaran, R., Wang, C., Siliciano, A.F., and Long, S.B. (2018). Cryo-EM structures of fungal and metazoan mitochondrial calcium uniporters. Nature *559*, 580–584.

Barnett, P., Arnold, R.S., Mezencev, R., Chung, L.W.K., Zayzafoon, M., and Odero-Marah, V. (2011). Snail-mediated regulation of reactive oxygen species in ARCaP human prostate cancer cells. Biochem. Biophys. Res. Commun. *404*, 34–39.

Basso, E., Fante, L., Fowlkes, J., Petronilli, V., Forte, M.A., and Bernardi, P. (2005). Properties of the Permeability Transition Pore in Mitochondria Devoid of Cyclophilin D. J. Biol. Chem. *280*, 18558–18561.

Baughman, J.M., Perocchi, F., Girgis, H.S., Plovanich, M., Belcher-Timme, C.A., Sancak, Y., Bao, X.R., Strittmatter, L., Goldberger, O., Bogorad, R.L., et al. (2011). Integrative genomics identifies MCU as an essential component of the mitochondrial calcium uniporter. Nature *476*, 341–345.

Baysal, B.E. (2003). On the association of succinate dehydrogenase mutations with hereditary paraganglioma. Trends Endocrinol. Metab. *14*, 453–459.

Berridge, M.J., Lipp, P., and Bootman, M.D. (2000). The versatility and universality of calcium signalling. Nat. Rev. Mol. Cell Biol. *1*, 11–21.

Boivin, B., Yang, M., and Tonks, N.K. (2010). Targeting the reversibly oxidized protein tyrosine phosphatase superfamily. Sci. Signal. *3*, pl2.

Breckpot, K., Dullaers, M., Bonehill, A., van Meirvenne, S., Heirman, C., de Greef, C., van der Bruggen, P., and Thielemans, K. (2003). Lentivirally transduced dendritic cells as a tool for cancer immunotherapy. J. Gene Med. *5*, 654–667.

Brini, M. (2008). Calcium-sensitive photoproteins. Methods *46*, 160–166.

Brini, M., Marsault, R., Bastianutto, C., Alvarez, J., Pozzan, T., and Rizzuto, R. (1995). Transfected Aequorin in the Measurement of Cytosolic Ca 2+ Concentration ([Ca 2+] c). J. Biol. Chem. *270*, 9896–9903.

Brookes, P.S., Yoon, Y., Robotham, J.L., Anders, M.W., and Sheu, S.-S. (2004). Calcium, ATP, and ROS: a mitochondrial love-hate triangle. Am. J. Physiol. Cell Physiol. *287*, C817-33.

Cannito, S., Novo, E., Compagnone, A., Valfrè di Bonzo, L., Busletta, C., Zamara, E., Paternostro, C., Povero, D., Bandino, A., Bozzo, F., et al. (2008). Redox mechanisms switch on hypoxia-dependent epithelial–mesenchymal transition in cancer cells. Carcinogenesis *29*, 2267–2278.

Chakraborty, P.K., Mustafi, S.B., Xiong, X., Dwivedi, S.K.D., Nesin, V., Saha, S., Zhang, M., Dhanasekaran, D., Jayaraman, M., Mannel, R., et al. (2017). MICU1 drives glycolysis and

chemoresistance in ovarian cancer. Nat. Commun. *8*, 14634.

Chiarugi, P., Pani, G., Giannoni, E., Taddei, L., Colavitti, R., Raugei, G., Symons, M., Borrello, S., Galeotti, T., and Ramponi, G. (2003). Reactive oxygen species as essential mediators of cell adhesion. J. Cell Biol. *161*, 933–944.

Chowdhury, R., Yeoh, K.K., Tian, Y.-M., Hillringhaus, L., Bagg, E.A., Rose, N.R., Leung, I.K.H., Li, X.S., Woon, E.C.Y., Yang, M., et al. (2011). The oncometabolite 2-hydroxyglutarate inhibits histone lysine demethylases. EMBO Rep. *12*, 463–469.

Christofk, H.R., Vander Heiden, M.G., Harris, M.H., Ramanathan, A., Gerszten, R.E., Wei, R., Fleming, M.D., Schreiber, S.L., and Cantley, L.C. (2008). The M2 splice isoform of pyruvate kinase is important for cancer metabolism and tumour growth. Nature *452*, 230–233.

Cobbold, P.H., and Bourne, P.K. (1984). Aequorin measurements of free calcium in single heart cells. Nature *312*, 444–446.

Csordás, G., Golenár, T., Seifert, E.L.L., Kamer, K.J.J., Sancak, Y., Perocchi, F., Moffat, C., Weaver, D., Perez, S. de la F.D.L.F., Bogorad, R., et al. (2013). MICU1 controls both the threshold and cooperative activation of the mitochondrial Ca2+ uniporter. Cell Metab. *17*, 976–987.

Curry, M.C., Peters, A.A., Kenny, P.A., Roberts-Thomson, S.J., and Monteith, G.R. (2013). Mitochondrial calcium uniporter silencing potentiates caspase-independent cell death in MDA-MB-231 breast cancer cells. Biochem. Biophys. Res. Commun. *434*, 695–700.

Davies, K.J. (1995). Oxidative stress: the paradox of aerobic life. Biochem. Soc. Symp. *61*, 1–31.

Davies, M.J. (2003). Singlet oxygen-mediated damage to proteins and its consequences. Biochem. Biophys. Res. Commun. *305*, 761–770.

DeBerardinis, R.J., Lum, J.J., Hatzivassiliou, G., and Thompson, C.B. (2008). The Biology of Cancer: Metabolic Reprogramming Fuels Cell Growth and Proliferation. Cell Metab. *7*, 11–20.

Disatnik, M.H., and Rando, T.A. (1999). Integrin-mediated muscle cell spreading. The role of protein kinase c in outside-in and inside-out signaling and evidence of integrin cross-talk. J. Biol. Chem. *274*, 32486–32492.

Dupuy, F., Tabariès, S., Andrzejewski, S., Dong, Z., Blagih, J., Annis, M.G., Omeroglu, A., Gao, D., Leung, S., Amir, E., et al. (2015). PDK1-Dependent Metabolic Reprogramming Dictates Metastatic Potential in Breast Cancer. Cell Metab. *22*, 577–589.

Ermakova, Y.G., Bilan, D.S., Matlashov, M.E., Mishina, N.M., Markvicheva, K.N., Subach, O.M., Subach, F. V., Bogeski, I., Hoth, M., Enikolopov, G., et al. (2014). Red fluorescent genetically encoded indicator for intracellular hydrogen peroxide. Nat. Commun. *5*, 1–9.

Fan, C., Fan, M., Orlando, B.J., Fastman, N.M., Zhang, J., Xu, Y., Chambers, M.G., Xu, X., Perry, K., Liao, M., et al. (2018). X-ray and cryo-EM structures of the mitochondrial calcium uniporter. Nature *559*, 575–579.

Felton, V.M., Borok, Z., and Willis, B.C. (2009). *N* -acetylcysteine inhibits alveolar epithelial-mesenchymal transition. Am. J. Physiol. Cell. Mol. Physiol. *297*, L805–L812.

Figueroa, M.E., Abdel-Wahab, O., Lu, C., Ward, P.S., Patel, J., Shih, A., Li, Y., Bhagwat, N., Vasanthakumar, A., Fernandez, H.F., et al. (2010). Leukemic IDH1 and IDH2 mutations result in a hypermethylation phenotype, disrupt TET2 function, and impair hematopoietic differentiation. Cancer Cell *18*, 553–567.

Fritz, V., and Fajas, L. (2010). Metabolism and proliferation share common regulatory pathways in cancer cells. Oncogene *29*, 4369–4377.

Gaude, E., and Frezza, C. (2014). Defects in mitochondrial metabolism and cancer. Cancer Metab. *2*, 10.

Giorgi, C., Romagnoli, A., Pinton, P., and Rizzuto, R. (2008). Ca2+ signaling, mitochondria and cell death. Curr. Mol. Med. *8*, 119–130.

Giorgi, C., Baldassari, F., Bononi, A., Bonora, M., De Marchi, E., Marchi, S., Missiroli, S., Patergnani, S., Rimessi, A., Suski, J.M., et al. (2012). Mitochondrial Ca(2+) and apoptosis. Cell Calcium *52*, 36–43.

Giorgi, C., Marchi, S., and Pinton, P. (2018). The machineries, regulation and cellular functions of mitochondrial calcium. Nat. Rev. Mol. Cell Biol. *19*, 713–730.

Görlach, A., Bertram, K., Hudecova, S., and Krizanova, O. (2015). Calcium and ROS: A mutual interplay. Redox Biol. *6*, 260–271.

Gorrini, C., Harris, I.S., Mak, T.W., discovery, T.M.-N. reviews D., and 2013, undefined (2013). Modulation of oxidative stress as an anticancer strategy. *12*, 931–947.

Grassian, A.R., Lin, F., Barrett, R., Liu, Y., Jiang, W., Korpal, M., Astley, H., Gitterman, D., Henley, T., Howes, R., et al. (2012). Isocitrate dehydrogenase (IDH) mutations promote a reversible ZEB1/microRNA (miR)-200-dependent epithelial-mesenchymal transition (EMT). J. Biol. Chem. *287*, 42180–42194.

Gu, L., Larson-Casey, J.L., and Carter, A.B. (2017). Macrophages utilize the mitochondrial calcium uniporter for profibrotic polarization. FASEB J. *31*, 3072–3083.

Guzy, R.D., Sharma, B., Bell, E., Chandel, N.S., and Schumacker, P.T. (2008). Loss of the SdhB, but Not the SdhA, Subunit of Complex II Triggers Reactive Oxygen Species-Dependent Hypoxia-Inducible Factor Activation and Tumorigenesis. Mol. Cell. Biol. *28*, 718–731.

Hall, D.D., Wu, Y., Domann, F.E., Spitz, D.R., and Anderson, M.E. (2014). Mitochondrial calcium uniporter activity is dispensable for MDA-MB-231 breast carcinoma cell survival. PLoS One *9*.

Han, M., Zhang, T., Yang, L., Wang, Z., Ruan, J., and Chang, X. (2016). Association between NADPH oxidase (NOX) and lung cancer: a systematic review and meta-analysis. J. Thorac. Dis. *8*, 1704–1711.

Hanahan, D., and Weinberg, R.A. (2000). The hallmarks of cancer. Cell *100*, 57–70.

Hanahan, D., Weinberg, R.A., Pan, K.H., Shay, J.W., Cohen, S.N., Taylor, M.B., Clarke, N.W., Jayson, G.C., Eshleman, J.R., Nowak, M.A., et al. (2011). Hallmarks of Cancer: The Next Generation. Cell *144*, 646–674.

Hartl, F.U., Pfanner, N., Nicholson, D.W., and Neupert, W. (1989). Mitochondrial protein import. Biochim. Biophys. Acta *988*, 1–45.

Head, J.F., Inouye, S., Teranishi, K., and Shimomura, O. (2000). The crystal structure of the photoprotein aequorin at 2.3 Å resolution. Nature *405*, 372–376.

Heiden, M.G. Vander, Cantley, L.C., Thompson, C.B., Mammalian, P., Exhibit, C., and Metabolism, A. (2009). Understanding the Warburg Effect : Cell Proliferation. Science (80-.).

Vander Heiden, M.G., Locasale, J.W., Swanson, K.D., Sharfi, H., Heffron, G.J., Amador-Noguez, D., Christofk, H.R., Wagner, G., Rabinowitz, J.D., Asara, J.M., et al. (2010). Evidence for an Alternative Glycolytic Pathway in Rapidly Proliferating Cells. Science (80-.). *329*,

1492–1499.

Hempel, N., and Trebak, M. (2017). Crosstalk between calcium and reactive oxygen species signaling in cancer. Cell Calcium *63*, 70–96.

Hirschi, M., Herzik Jr, M.A., Wie, J., Suo, Y., Borschel, W.F., Ren, D., Lander, G.C., and Lee, S.-Y. (2017). Cryo-electron microscopy structure of the lysosomal calcium-permeable channel TRPML3. Nature *550*, 411–414.

Hong, Z., Chen, K.-H., DasGupta, A., Potus, F., Dunham-Snary, K., Bonnet, S., Tian, L., Fu, J., Breuils-Bonnet, S., Provencher, S., et al. (2017). MicroRNA-138 and MicroRNA-25 Down-regulate Mitochondrial Calcium Uniporter, Causing the Pulmonary Arterial Hypertension Cancer Phenotype. Am. J. Respir. Crit. Care Med. *195*, 515–529.

Hsu, P.P., and Sabatini, D.M. (2008). Cancer Cell Metabolism: Warburg and Beyond. Cell *134*, 703–707.

Hu, C.-T., Wu, J.-R., Cheng, C.-C., Wang, S., Wang, H.-T., Lee, M.-C., Wang, L.-J., Pan, S.-M., Chang, T.-Y., and Wu, W.-S. (2011). Reactive oxygen species-mediated PKC and integrin signaling promotes tumor progression of human hepatoma HepG2. Clin. Exp. Metastasis *28*, 851–863.

Kamer, K.J., and Mootha, V.K. (2014). MICU1 and MICU2 play non redundant roles in the
regulation of the mitochondrial calcium uniporter. EMBO Rep. *15*, 299–307.

Koppenol, W.H., Bounds, P.L., and Dang, C. V. (2011). Otto Warburg's contributions to current concepts of cancer metabolism. Nat. Rev. Cancer *11*, 325–337.

LeBleu, V.S., O'Connell, J.T., Gonzalez Herrera, K.N., Wikman, H., Pantel, K., Haigis, M.C., de Carvalho, F.M., Damascena, A., Domingos Chinen, L.T., Rocha, R.M., et al. (2014). PGC-1α mediates mitochondrial biogenesis and oxidative phosphorylation in cancer cells to promote metastasis. Nat. Cell Biol. *16*, 992–1003.

Lee, E.K., Jeon, W.-K., Chae, M.Y., Hong, H.-Y., Lee, Y.S., Kim, J.H., Kwon, J.Y., Kim, B.-C., and Park, S.H. (2010). Decreased expression of glutaredoxin 1 is required for transforming growth factor-β1-mediated epithelial–mesenchymal transition of EpRas mammary epithelial cells. Biochem. Biophys. Res. Commun. *391*, 1021–1027.

Long, J., Zhang, Z.-B., Liu, Z., Xu, Y.-H., and Ge, C.-L. (2015). Loss of Heterozygosity at the Calcium Regulation Gene Locus on Chromosome 10q in Human Pancreatic Cancer. Asian Pacific J. Cancer Prev. *16*, 2489–2493.

López-Soto, A., Gonzalez, S., Smyth, M.J., and Galluzzi, L. (2017). Control of Metastasis by NK Cells. Cancer Cell *32*, 135–154.

Loubiere, C., Clavel, S., Gilleron, J., Harisseh, R., Fauconnier, J., Ben-Sahra, I., Kaminski, L., Laurent, K., Herkenne, S., Lacas-Gervais, S., et al. (2017). The energy disruptor metformin targets mitochondrial integrity via modification of calcium flux in cancer cells. Sci. Rep. *7*, 5040.

Mahdi, M.H. Ben, Andrieu, V., and Pasquier, C. (2001). Focal Adhesion Kinase Regulation by Oxidative Stress in Different Cell Types. IUBMB Life *50*, 291–299.

Mallilankaraman, K., Doonan, P., Cárdenas, C., Chandramoorthy, H.C., Müller, M., Miller, R., Hoffman, N.E., Gandhirajan, R.K., Molgó, J., Birnbaum, M.J., et al. (2012). MICU1 is an essential gatekeeper for MCU-mediated mitochondrial Ca(2+) uptake that regulates cell survival. Cell *151*, 630–644.

Mammucari, C., Gherardi, G., Zamparo, I., Raffaello, A., Boncompagni, S., Chemello,

F., Cagnin, S., Braga, A., Zanin, S., Pallafacchina, G., et al. (2015). The mitochondrial calcium uniporter controls skeletal muscle trophism in vivo. Cell Rep. *10*, 1269–1279.

Mammucari, C., Gherardi, G., and Rizzuto, R. (2017). Structure, Activity Regulation, and Role of the Mitochondrial Calcium Uniporter in Health and Disease. Front. Oncol. *7*, 139.

Mammucari, C., Raffaello, A., Vecellio Reane, D., Gherardi, G., De Mario, A., and Rizzuto, R. (2018). Mitochondrial calcium uptake in organ physiology: from molecular mechanism to animal models. Pflügers Arch. - Eur. J. Physiol. 1165–1179.

Mannella, C.A. (2006). Structure and dynamics of the mitochondrial inner membrane cristae. Biochim. Biophys. Acta - Mol. Cell Res. *1763*, 542–548.

Marchi, S., Lupini, L., Patergnani, S., Rimessi, A., Missiroli, S., Bonora, M., Bononi, A., Corrà, F., Giorgi, C., De Marchi, E., et al. (2013). Downregulation of the mitochondrial calcium uniporter by cancer-related miR-25. Curr. Biol. *23*, 58–63.

Mayers, J.R., Torrence, M.E., Danai, L. V., Papagiannakopoulos, T., Davidson, S.M., Bauer, M.R., Lau, A.N., Ji, B.W., Dixit, P.D., Hosios, A.M., et al. (2016). Tissue of origin dictates branched-chain amino acid metabolism in mutant Kras-driven cancers. Science (80-.). *353*, 1161–1165.

McCormack, J.G., Halestrap, A.P., and Denton, R.M. (1990). Role of calcium ions in regulation of mammalian intramitochondrial metabolism. Physiol. Rev. *70*, 391–425.

Mitchell, K.J., Pinton, P., Varadi, A., Tacchetti, C., Ainscow, E.K., Pozzan, T., Rizzuto, R., and Rutter, G.A. (2001). Dense core secretory vesicles revealed as a dynamic Ca2+ store in neuroendocrine cells with a vesicle-associated membrane protein aequorin chimaera. J. Cell Biol. *155*, 41.

Moloney, J.N., and Cotter, T.G. (2018). ROS signalling in the biology of cancer. Semin. Cell Dev. Biol. *80*, 50–64.

Montero, M., Brini, M., Marsault, R., Alvarez, J., Sitia, R., Pozzan, T., and Rizzuto, R. (1995). Monitoring dynamic changes in free Ca2+ concentration in the endoplasmic reticulum of intact cells. *14*.

Murphy, M.P. (2009). How mitochondria produce reactive oxygen species. Biochem. J. *417*, 1–13.

Nishikawa, M. (2008). Reactive oxygen species in tumor metastasis. Cancer Lett. *266*, 53–59.

Nobes, C.D., and Hall, A. (1999). Rho GTPases Control Polarity, Protrusion, and Adhesion during Cell Movement. J. Cell Biol. *144*, 1235–1244.

Nogueira, V., Park, Y., Chen, C.-C., Xu, P.-Z., Chen, M.-L., Tonic, I., Unterman, T., and Hay, N. (2008). Akt Determines Replicative Senescence and Oxidative or Oncogenic Premature Senescence and Sensitizes Cells to Oxidative Apoptosis. Cancer Cell *14*, 458–470.

Pagliarini, D.J., Calvo, S.E., Chang, B., Sheth, S.A., Vafai, S.B., Ong, S.-E., Walford, G.A., Sugiana, C., Boneh, A., Chen, W.K., et al. (2008). A mitochondrial protein compendium elucidates complex I disease biology. Cell *134*, 112–123.

Pan, X., Liu, J., Nguyen, T., Liu, C., Sun, J., Teng, Y., Fergusson, M.M., Rovira, I.I., Allen, M., Springer, D.A., et al. (2013). The physiological role of mitochondrial calcium revealed by mice lacking the mitochondrial calcium uniporter. Nat. Cell Biol. *15*, 1464–1472.

Patron, M., Checchetto, V., Raffaello, A., Teardo, E., Vecellio Reane, D., Mantoan, M., Granatiero, V., Szabò, I., De Stefani, D., and Rizzuto, R. (2014a). MICU1 and MICU2 Finely

Tune the Mitochondrial Ca2+ Uniporter by Exerting Opposite Effects on MCU Activity. Mol. Cell *53*, 726–737.

Patron, M., Checchetto, V., Raffaello, A., Teardo, E., Vecellio Reane, D., Mantoan, M., Granatiero, V., Szabò, I., De Stefani, D., and Rizzuto, R. (2014b). MICU1 and MICU2 finely tune the mitochondrial Ca2+ uniporter by exerting opposite effects on MCU activity. Mol. Cell *53*, 726–737.

Patron, M., Granatiero, V., Espino, J., Rizzuto, R., and De Stefani, D. (2019). MICU3 is a tissue-specific enhancer of mitochondrial calcium uptake. Cell Death Differ. *26*, 179–195.

Pavlova, N.N., and Thompson, C.B. (2016). The Emerging Hallmarks of Cancer Metabolism. Cell Metab. *23*, 27–47.

Pelicano, H., Carney, D., and Huang, P. (2004). ROS stress in cancer cells and therapeutic implications. Drug Resist. Updat. *7*, 97–110.

Perocchi, F., Gohil, V.M., Girgis, H.S., Bao, X.R., McCombs, J.E., Palmer, A.E., and Mootha, V.K. (2010). MICU1 encodes a mitochondrial EF hand protein required for Ca(2+) uptake. Nature *467*, 291–296.

Pfeiffer, T., Schuster, S., and Bonhoeffer, S. (2001). Cooperation and competition in the evolution of ATP-producing pathways. Science (80-.). *292*, 504–507.

Pinton, P., Ferrari, D., Rapizzi, E., Di Virgilio, F., Pozzan, T., and Rizzuto, R. (2001). The Ca2+ concentration of the endoplasmic reticulum is a key determinant of ceramide-induced apoptosis: significance for the molecular mechanism of Bcl-2 action. EMBO J. *20*, 2690–2701.

Plovanich, M., Bogorad, R.L., Sancak, Y., Kamer, K.J., Strittmatter, L., Li, A.A., Girgis, H.S., Kuchimanchi, S., De Groot, J., Speciner, L., et al. (2013). MICU2, a Paralog of MICU1, Resides within the Mitochondrial Uniporter Complex to Regulate Calcium Handling. PLoS One *8*, e55785.

Porporato, P.E., Payen, V.L., Pérez-Escuredo, J., De Saedeleer, C.J., Danhier, P., Copetti, T., Dhup, S., Tardy, M., Vazeille, T., Bouzin, C., et al. (2014). A mitochondrial switch promotes tumor metastasis. Cell Rep. *8*, 754–766.

Prudent, J., Popgeorgiev, N., Bonneau, B., Thibaut, J., Gadet, R., Lopez, J., Gonzalo, P., Rimokh, R., Manon, S., Houart, C., et al. (2013). Bcl-wav and the mitochondrial calcium uniporter drive gastrula morphogenesis in zebrafish. Nat. Commun. *4*, 1–15.

Racker, E. (1976). Why do tumor cells have a high aerobic glycolysis? J. Cell. Physiol. *89*, 697–700.

Radisky, D.C., Levy, D.D., Littlepage, L.E., Liu, H., Nelson, C.M., Fata, J.E., Leake, D., Godden, E.L., Albertson, D.G., Angela Nieto, M., et al. (2005). Rac1b and reactive oxygen species mediate MMP-3-induced EMT and genomic instability. Nature *436*, 123–127.

Raffaello, A., De Stefani, D., Sabbadin, D., Teardo, E., Merli, G., Picard, A., Checchetto, V., Moro, S., Szabò, I., and Rizzuto, R. (2013). The mitochondrial calcium uniporter is a multimer that can include a dominant-negative pore-forming subunit. EMBO J. *32*, 2362–2376.

Ren, T., Zhang, H., Wang, J., Zhu, J., Jin, M., Wu, Y., Guo, X., Ji, L., Huang, Q., Zhang, H., et al. (2017). MCU-dependent mitochondrial Ca 2+ inhibits NAD +/SIRT3/SOD2 pathway to promote ROS production and metastasis of HCC cells. Oncogene *36*, 5897–5909.

Rizzuto, R., Simpson, A.W., Brini, M., and Pozzan, T. (1992). Rapid changes of mitochondrial Ca2+ revealed by specifically targeted recombinant aequorin. Nature *358*, 325–327.

Sabharwal, S.S., and Schumacker, P.T. (2014). Mitochondrial ROS in cancer: initiators, amplifiers or an Achilles' heel? Nat. Rev. Cancer *14*, 709–721.

Sancak, Y., Markhard, A.L., Kitami, T., Kovács-Bogdán, E., Kamer, K.J., Udeshi, N.D., Carr, S.A., Chaudhuri, D., Clapham, D.E., Li, A.A., et al. (2013). EMRE is an essential component of the mitochondrial calcium uniporter complex. Science *342*, 1379–1382.

Schindelin, J., Arganda-Carreras, I., Frise, E., Kaynig, V., Longair, M., Pietzsch, T., Preibisch, S., Rueden, C., Saalfeld, S., Schmid, B., et al. (2012). Fiji: an open-source platform for biological-image analysis. Nat. Methods *9*, 676–682.

Sciacovelli, M., and Frezza, C. (2017). Metabolic reprogramming and epithelial-to-mesenchymal transition in cancer. FEBS J. *284*, 3132–3144.

Selak, M.A., Armour, S.M., MacKenzie, E.D., Boulahbel, H., Watson, D.G., Mansfield, K.D., Pan, Y., Simon, M.C., Thompson, C.B., and Gottlieb, E. (2005). Succinate links TCA cycle dysfunction to oncogenesis by inhibiting HIF-alpha prolyl hydroxylase. Cancer Cell *7*, 77–85.

De Stefani, D., Raffaello, A., Teardo, E., Szabò, I., and Rizzuto, R. (2011). A forty-kilodalton protein of the inner membrane is the mitochondrial calcium uniporter. Nature *476*, 336–340.

De Stefani, D., Rizzuto, R., and Pozzan, T. (2016). Enjoy the Trip: Calcium in Mitochondria Back and Forth. Annu. Rev. Biochem. *85*, 161–192.

Taddei, M.L., Parri, M., Mello, T., Catalano, A., Levine, A.D., Raugei, G., Ramponi, G., and Chiarugi, P. (2007). Integrin-mediated cell adhesion and spreading engage different sources of reactive oxygen species. Antioxid. Redox Signal. *9*, 469–481.

Tan, B.L., Norhaizan, M.E., Liew, W.-P.-P., and Sulaiman Rahman, H. (2018). Antioxidant and Oxidative Stress: A Mutual Interplay in Age-Related Diseases. Front. Pharmacol. *9*, 1162.

Tomar, D., Rajan, S., Stathopulos, P.B., Dong, Z., Shanmughapriya, S., Tomar, D., Siddiqui, N., and Lynch, S. (2017). Mitochondrial Ca 2 + Uniporter Is a Mitochondrial Luminal Redox Sensor that Augments MCU Channel Article Mitochondrial Ca 2 + Uniporter Is a Mitochondrial Luminal Redox Sensor that Augments MCU Channel Activity. *65*, 1–15.

Tomlinson, I.P.M., Alam, N.A., Rowan, A.J., Barclay, E., Jaeger, E.E.M., Kelsell, D., Leigh, I., Gorman, P., Lamlum, H., Rahman, S., et al. (2002). Germline mutations in FH predispose to dominantly inherited uterine fibroids, skin leiomyomata and papillary renal cell cancer. Nat. Genet. *30*, 406–410.

Tosatto, A., Sommaggio, R., Kummerow, C., Bentham, R.B., Blacker, T.S., Berecz, T., Duchen, M.R., Rosato, A., Bogeski, I., Szabadkai, G., et al. (2016). The mitochondrial calcium uniporter regulates breast cancer progression via HIF-1a. EMBO Mol Med *8*, 569–585.

Tretter, L., and Adam-Vizi, V. (2004). Generation of Reactive Oxygen Species in the Reaction Catalyzed by -Ketoglutarate Dehydrogenase. J. Neurosci. *24*, 7771–7778.

Tretter, L., Takacs, K., Kövér, K., and Adam-Vizi, V. (2007). Stimulation of H2O2 generation by calcium in brain mitochondria respiring on α-glycerophosphate. J. Neurosci. Res. *85*, 3471–3479.

Tsai, F.C., Seki, A., Yang, H.W., Hayer, A., Carrasco, S., Malmersjö, S., Meyer, T. (2014). A polarized Ca2+, diacylglycerol and STIM1 signalling system regulates directed cell migration. Nature.Com. 16(2):133-44

Vultur, A., Gibhardt, C.S., Stanisz, H., and Bogeski, I. (2018). The role of the

mitochondrial calcium uniporter (MCU) complex in cancer. Pflugers Arch. Eur. J. Physiol. *470*, 1149–1163.

Vyas, S., Zaganjor, E., and Haigis, M.C. (2016). Mitochondria and Cancer. Cell. ;166(3):555-566

Wang, P. (2014). Chloride intracellular channel 1 regulates colon cancer cell migration and invasion through ROS/ERK pathway. World J. Gastroenterol. *20*, 2071.

Wang, Y., Wang, F., Wang, R., Zhao, P., and Xia, Q. (2015). 2A self-cleaving peptide-based multi-gene expression system in the silkworm Bombyx mori. Sci. Rep. *5*, 1–10.

Warburg, O. (1956). On the Origin of Cancer Cells. Science *123*, 309–314.

Warburg, O., Wind, F., and Negelein, E. (1927). I . Killing-Off of Tumor Cells in Vitro . J. Gen. Physiol. *8*, 519–530.

Weinhouse, S. (1976). The Warburg hypothesis fifty years later. Z. Krebsforsch. Klin. Onkol. Cancer Res. Clin. Oncol. *87*, 115–126.

Werner, E., and Werb, Z. (2002). Integrins engage mitochondrial function for signal transduction by a mechanism dependent on Rho GTPases. J. Cell Biol. *158*, 357–368.

Wiel, C., Lallet-Daher, H., Gitenay, D., Gras, B., Le Calvé, B., Augert, A., Ferrand, M., Prevarskaya, N., Simonnet, H., Vindrieux, D., et al. (2014). Endoplasmic reticulum calcium release through ITPR2 channels leads to mitochondrial calcium accumulation and senescence. Nat. Commun. *5*, 3792.

Wu, W.-S. (2006). The signaling mechanism of ROS in tumor progression. Cancer Metastasis Rev. *25*, 695–705.

Xu, S., and Chisholm, A.D. (2014). Article C . elegans Epidermal Wounding Induces a Mitochondrial ROS Burst that Promotes Wound Repair. Dev. Cell *31*, 48–60.

Yamazaki, S., Miyoshi, N., Kawabata, K., Yasuda, M., and Shimoi, K. (2014). Quercetin-3-O-glucuronide inhibits noradrenaline-promoted invasion of MDA-MB-231 human breast cancer cells by blocking β2-adrenergic signaling. Arch. Biochem. Biophys. *557*, 18–27.

Yang, M., and Pollard, P.J. (2013). Succinate: A New Epigenetic Hacker. Cancer Cell *23*, 709–711.

Yang, Y., Karakhanova, S., Hartwig, W., D'Haese, J.G., Philippov, P.P., Werner, J., and Bazhin, A. V. (2016). Mitochondria and Mitochondrial ROS in Cancer: Novel Targets for Anticancer Therapy. J. Cell. Physiol. *231*, 2570–2581.

Yoo, J., Wu, M., Yin, Y., Herzik, M.A., Lander, G.C., and Lee, S.-Y. (2018). Cryo-EM structure of a mitochondrial calcium uniporter. Science 361(6401):506-511

Zampieri, S., Mammucari, C., Romanello, V., Barberi, L., Pietrangelo, L., Fusella, A., Mosole, S., Gherardi, G., Höfer, C., Löfler, S., et al. (2016). Physical exercise in aging human skeletal muscle increases mitochondrial calcium uniporter expression levels and affects mitochondria dynamics. Physiol. Rep. *4*, e13005.

Zhang, J., Nuebel, E., Daley, G.Q., Koehler, C.M., and Teitell, M.A. (2012). Metabolic Regulation in Pluripotent Stem Cells during Reprogramming and Self-Renewal. Cell Stem Cell *11*, 589–595.

Zhou, X., Ren, Y., Kong, L., Cai, G., Sun, S., Song, W., Wang, Y., Jin, R., Qi, L., Mei, M., et al. (2015). Targeting EZH2 regulates tumor growth and apoptosis through modulating mitochondria dependent cell-death pathway in HNSCC. Oncotarget *6*, 33720–33732.